

A DWARF IRREGULAR GALAXY AT THE EDGE OF THE LOCAL GROUP: STELLAR POPULATIONS AND DISTANCE OF IC 5152¹

ALBERT A. ZIJLSTRA² AND DANTE MINNITI^{3,4}

Received 1998 July 21; accepted 1998 December 11

ABSTRACT

We have obtained V - and I -band photometry for about 700 stars in the field of the dwarf irregular galaxy IC 5152, previously considered a possible member of the Local Group. Deep VI color-magnitude diagrams are presented of the main body of this galaxy and of a nearby field. We infer a distance by comparison with the VI color-magnitude diagrams of similar galaxies and with theoretical isochrones. The distance modulus to IC 5152 is found to be $m - M_0 = 26.15 \pm 0.2$, adopting $E(V-I) = 0$. This distance of $D = 1.7$ Mpc implies that IC 5152 is not a certain member of the Local Group. We also construct a deep optical luminosity function. By comparison with theoretical isochrones, we find a metallicity $Z \approx 0.002$, which is lower than previous estimates. Using this metallicity and distance, IC 5152 now fits the metallicity-luminosity relation for dwarf galaxies. The youngest stars in the field studied have an age of $\sim 10^7$ Gyr, and there is a substantial population of stars with $\log t > 7.8 - 8$ yr. The central region of IC 5152 is an active site of star formation, as found by comparing our optical photometry with *Hubble Space Telescope* ultraviolet images. Several candidate globular clusters are found, as well as a candidate for a potential nucleus.

Key words: galaxies: individual (IC 5152, IRAS 21594–51, ESO 237-27) — galaxies: irregular — galaxies: stellar content — Galaxy: formation — Local Group

1. INTRODUCTION

Dwarf galaxies are the most numerous galaxies in the Local Group and nearby universe. Their evolution shows evidence of being affected by their environment, with gas-poor dwarf spheroidals mainly occurring near larger galaxies, and gas-rich dwarf irregulars being more common in relative isolation (e.g., van den Bergh 1994a). In return, dwarf galaxies may themselves have contributed to the formation of spiral galaxies such as the Milky Way, because gravitational clustering on progressively larger scales can have played an important role in the formation of large galaxies (White & Rees 1978). In this context, it is important to study the isolated dwarfs that live in low-density environments, distant enough from other major galaxies to have remained unperturbed during a Hubble time.

The Sdm IV–V galaxy IC 5152 is one such system, previously considered to be a member of the Local Group. Sandage (1986) quotes a distance modulus of $m - M_0 = 24.9$ from the brightest supergiants, equivalent to $D = 1.58$ Mpc. Recently, however, van den Bergh (1994a) pointed out that the distances measured, ranging from 1.5 to 3.0 Mpc (Bottinelli et al. 1984), are too uncertain to secure membership. A summary of parameters for this galaxy is given in Table 1. Despite the fact that IC 5152 is listed as one of the galaxies most easily resolved into stars (Sandage & Bedke

1985), there is no previous color-magnitude diagram of this galaxy, and its past star formation history is unknown (Mateo 1998; Grebel 1998). A very bright star in front of this galaxy (HD 209142, with $V = 7.9$) makes it difficult to obtain deep exposures (see Fig. 1). Bedding et al. (1997) took advantage of the bright star in the field as a reference for using an adaptive optics system in order to resolve the galaxy into stars. They could only detect a few stars at very faint levels and concluded that this galaxy must be more distant than previously thought.

In this paper, we discuss the stellar populations of the isolated dwarf irregular galaxy IC 5152, based on VI photometry (down to $I = 23.0$) covering a large area to the southeast of the main body of this galaxy. From the VI color-magnitude diagram and a deep luminosity function, we measure a distance of 1.7 Mpc to IC 5152, which places it at the edge of the Local Group.

The observations of IC 5152, data reductions, and photometry are described in § 2. The resulting color-magnitude diagrams and luminosity functions are given in § 3, along with a discussion about reddening. Fundamental parameters of IC 5152 (metallicity, age, and distance) are determined in § 4. Other population tracers (star clusters, carbon stars, H II regions, planetary nebulae, Cepheid variables, CO and H I observations) are reviewed in § 5. The possible association of IC 5152 with either the Local Group or the Sculptor Group is discussed in § 6. Finally, the conclusions of this work are summarized in § 7.

2. DATA

2.1. Observations and Reductions

The observations of IC 5152 were obtained during the night of 1995 September 5 as part of a long-term monitoring program of the variable stars in several galaxies (Zijlstra, Minniti, & Brewer 1997). We used the red arm (RILD mode) of the ESO Multi-Mode Instrument (EMMI) at the New Technology Telescope (NTT) in La Silla, operated in active remote control (Zijlstra et al. 1997) from ESO

¹ Based on observations collected at the La Silla Observatory, operated by the European Southern Observatory, and on archival data of the NASA/ESA *Hubble Space Telescope*, which is operated by the Association of Universities for Research in Astronomy, Inc., under NASA contract NAS 5-26555.

² Department of Physics, UMIST, P.O. Box 88, Manchester M60 1QD, UK; aaz@iapetus.phy.umist.ac.uk.

³ Lawrence Livermore National Laboratory, Institute of Geophysics and Planetary Physics, P.O. Box 808, Mail Stop L-413, Livermore, CA 94550; dminniti@llnl.gov.

⁴ Departamento de Astronomía, Pontificia Universidad Católica, Department of Astronomy and Astrophysics, Casilla 104, Santiago 22, Chile.

TABLE 1
SUMMARY OF PARAMETERS FOR IC 5152

Parameter	Value	Reference
α, δ (J2000.0)	22 02 41.22, -51 17 47.9	4
(l, b)	343°.91, -50°.19	4
Distance modulus	26.15 ± 0.20	1
Distance	1.7 Mpc	1
Type	Sdm IV-V	4
M_B	-14.8	2
$E(V-I)$	0.00	1
b/a_{disk}	0.6	4
V_{LG}	+53 km s ⁻¹	2
Inclination	55°	2
Diameter	2.1 kpc	2
Z_{disk}	0.002	3

NOTE.—Units of right ascension are hours, minutes, and seconds, and units of declination are degrees, arcminutes, and arcseconds.

REFERENCES.—(1) This work. (2) Huchtmeier & Richter 1986. (3) Skillman et al. 1989a, 1989b. (4) Sandage & Bedke 1985.

headquarters in Garching, Germany. The weather was photometric. We used the 2048 × 2048 Tek CCD, with a scale of 0''.268 pixel⁻¹.

The observations of this galaxy consist of pairs of frames with exposure times of 900 s in I (air mass 1.1) and 1800 s in V (air mass 1.1). A total of five standards of Landolt (1992) were observed during the night in order to calibrate our photometry.

The reductions of the CCD frames were carried out following standard procedures, using the package CCDRED within the IRAF environment. The pairs of images in each filter were combined, the final FWHM of stellar images being 0''.8 in V and I .

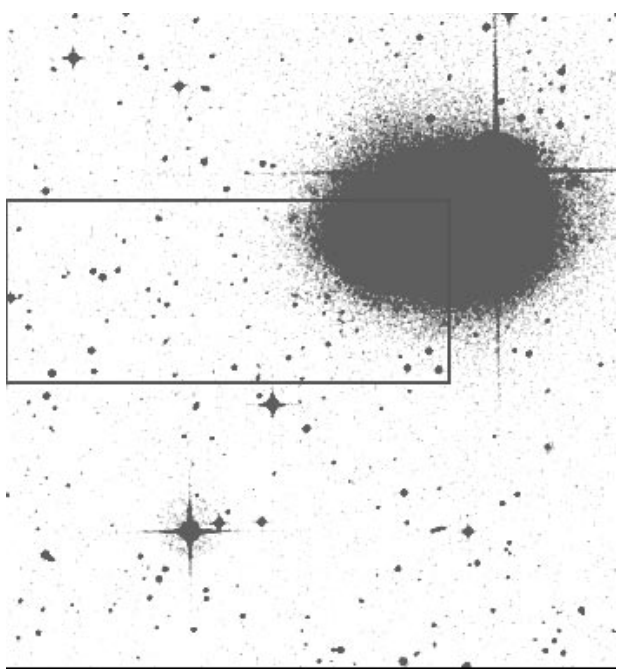


FIG. 1.—Image of IC 5152 from POSS. North is up, and east to the left, with a scale of 20' × 20'. The field studied in this paper is indicated by the rectangle. At the distance of IC 5152, 1' = 0.5 kpc. Note the spikes of the bright star HD 209142, with $V = 7.9$, overlapped on the northwest corner of this galaxy.

Because of the superposition of a very bright foreground star (HD 209142 = SAO 247284, with $V = 7.9$, $B-V = 0.1$; see Fig. 1), this galaxy has not been observed systematically before. We pointed the telescope away from the bright star, covering the southeast corner of IC 5152. Nonetheless, additional reflections of this star in the telescope and instrument optics still cause a residual gradient in the background, which ultimately presents a problem when flat-fielding the data. Therefore, we adopt a conservative systematic error of 0.1 mag in all the photometry derived here. Also, even though the field covers 8'.5 × 9', we use only a region of 9' × 3', covering about one-quarter of this galaxy plus a large enough neighboring field for comparison (Fig. 2).

2.2. The Photometry

The photometric transformations to the standard system were done following the procedure described by Minniti & Zijlstra (1997). These transformations reproduce the magnitudes of the standard stars with an rms of 0.02 in V and 0.03 in I .

The photometric measurements were performed within the IRAF environment using DAOPHOT II, which is an improved version of the original DAOPHOT package developed by Stetson (1987). In particular, DAOPHOT II can accommodate a spatially varying point-spread function across the field. All stars in the field of IC 5152 with more than 4 σ above the background in the V and I frames were located and their magnitudes measured by fitting an empirical point-spread function. The position of these objects is plotted schematically in Figure 3. Figure 4 shows the DAOPHOT errors as functions of V - and I -band magnitudes, excluding the flat-fielding uncertainty. The resulting limiting magnitudes at 4 σ are $V = 24$ and $I = 23$.

The completeness in the photometry varies across the field. As expected, the completeness is worse in the more crowded disk region of IC 5152 ($C \sim 75\%$) than in the outer regions ($C \sim 90\%$). However, the present photometry is sufficiently deep that none of our results will depend on the completeness of the sample at the faintest magnitudes. Most of the stars detected in the I -frames down to $I = 23.0$ are concentrated in the disk of the galaxy. IC 5152 is reasonably face-on, with an inclination $i = 55^\circ$ (Hutchmeier & Richter 1986).

The photometry of the IC 5152 disk field is listed in Table 2. Columns (1) and (2) give the star positions in pixels. With the scale of 0''.268 pixel⁻¹, 1' is equivalent to 0.5 kpc at the distance of $D = 1.7$ Mpc. Columns (3)–(6) give the V and I magnitudes, with their respective errors. Finally, column (7) lists the $V-I$ colors.

3. THE COLOR-MAGNITUDE DIAGRAMS AND LUMINOSITY FUNCTION

3.1. The Color-Magnitude Diagrams

Deep optical color-magnitude diagrams are the main tools to study the stellar content of resolved galaxies (e.g., Greggio et al. 1993; Lee 1993; Tosi 1994; Tolstoy 1995; Tolstoy & Saha 1996; Marconi, Matteucci, & Tosi 1994; Gallart et al. 1994; Gallart, Aparicio, & Vinchez 1996; Dohm-Palmer et al. 1997). The lack of a deep color-magnitude diagram for IC 5152 has caused the star formation history of this galaxy to remain unknown (see Mateo

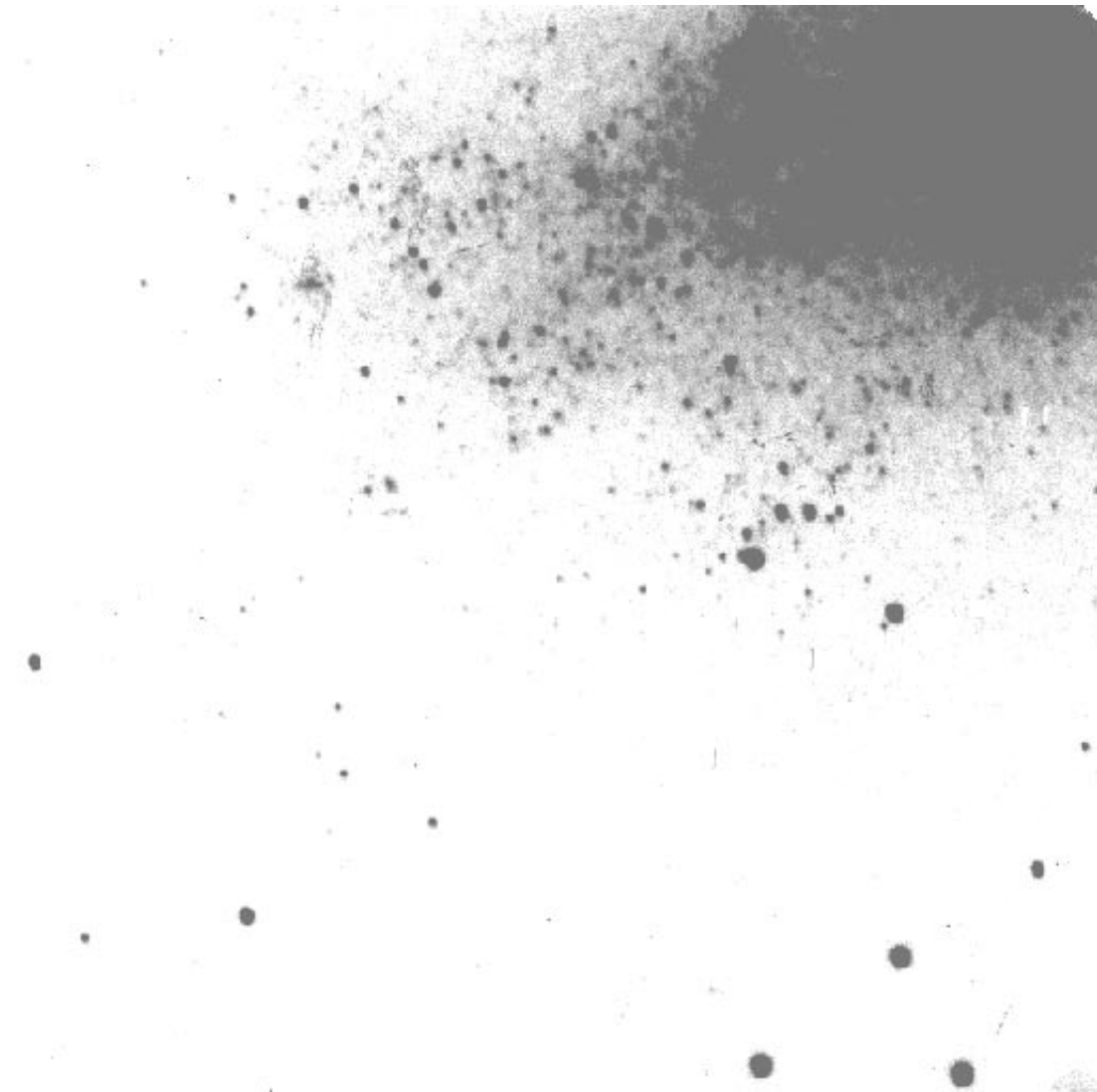


FIG. 2.—Portion of the V image of IC 5152 taken at the NTT. North is up, and east to the left, with a field of about $3' \times 3'$, equivalent to about 1.5 kpc on a side.

1998; Grebel 1998). Some photographic photometry exists in the literature: Sandage (1986) quotes distance results from photometric measurements of the brightest giants in this galaxy.

Figure 5 shows the first color-magnitude diagrams based on CCD photometry of the dwarf galaxy IC 5152. It shows the I versus $V-I$ and V versus $V-I$ color-magnitude dia-

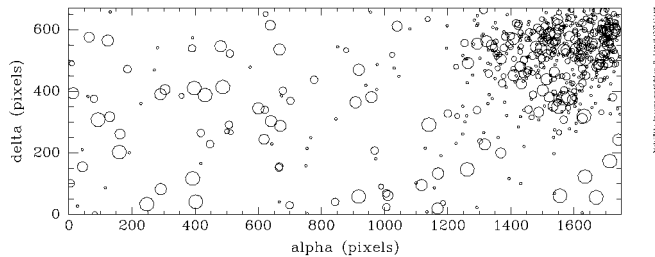


FIG. 3.—Map of all the stars detected in the field of IC 5152 taken with the NTT. The sizes of the circles are proportional to the I -band magnitudes of the stars. The scale is $0''.268 \text{ pixel}^{-1}$. North is up, and east is to the left.

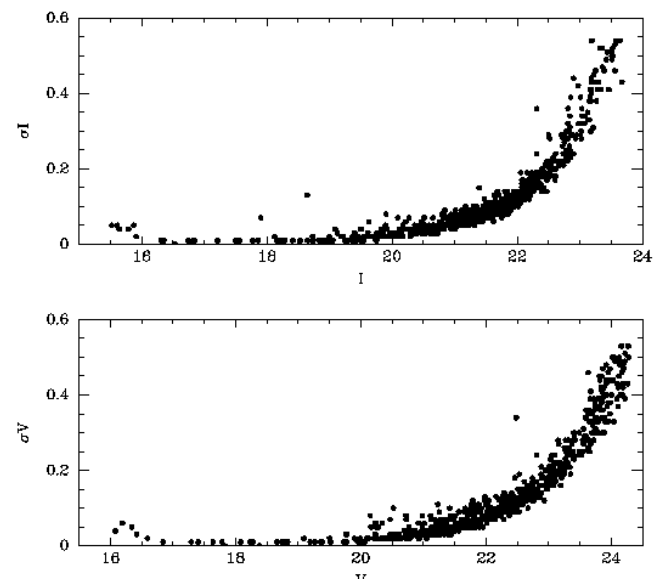


FIG. 4.—DAOPHOT V - and I -band errors as function of magnitude

TABLE 2
PHOTOMETRY OF IC 5152

<i>X</i> (1)	<i>Y</i> (2)	<i>V</i> (3)	σ_V (4)	<i>I</i> (5)	σ_I (6)	<i>V</i> – <i>I</i> (7)	<i>X</i> (1)	<i>Y</i> (2)	<i>V</i> (3)	σ_V (4)	<i>I</i> (5)	σ_I (6)	<i>V</i> – <i>I</i> (7)
1136.38.....	633.89	22.32	0.09	21.28	0.06	1.04	1346.61.....	541.23	20.71	0.03	20.82	0.04	-0.11
1140.38.....	291.20	18.75	0.00	16.53	0.00	2.22	1348.74.....	554.62	22.51	0.11	22.57	0.23	-0.07
1149.74.....	172.46	23.04	0.16	22.45	0.19	0.58	1350.00.....	441.29	21.44	0.03	21.71	0.10	-0.27
1156.24.....	544.71	23.03	0.19	23.51	0.50	-0.48	1350.44.....	622.25	22.46	0.12	22.31	0.24	0.15
1169.46.....	133.12	20.51	0.02	18.41	0.01	2.10	1351.51.....	521.07	21.97	0.08	21.05	0.05	0.92
1178.83.....	190.40	23.30	0.24	21.55	0.09	1.75	1352.04.....	560.85	21.70	0.07	21.41	0.07	0.28
1193.98.....	303.99	23.32	0.26	23.01	0.29	0.31	1354.80.....	511.74	22.45	0.12	21.39	0.07	1.07
1196.11.....	539.47	23.79	0.39	22.73	0.24	1.06	1354.81.....	602.23	23.31	0.22	22.74	0.29	0.57
1197.83.....	612.09	22.48	0.11	21.50	0.08	0.98	1356.98.....	525.62	20.89	0.03	21.18	0.06	-0.29
1200.12.....	327.34	22.56	0.13	20.29	0.02	2.27	1358.19.....	474.07	22.21	0.08	21.18	0.06	1.03
1203.06.....	507.52	21.55	0.05	21.62	0.08	-0.07	1359.51.....	250.21	22.87	0.14	22.21	0.13	0.66
1204.22.....	636.65	23.81	0.45	22.42	0.15	1.39	1362.96.....	518.61	20.87	0.04	21.40	0.08	-0.53
1205.33.....	651.59	24.16	0.53	21.91	0.10	2.25	1364.68.....	556.17	22.20	0.10	22.29	0.16	-0.09
1212.77.....	639.74	21.78	0.05	22.02	0.11	-0.24	1366.29.....	355.02	24.16	0.48	23.15	0.33	1.01
1217.85.....	173.72	23.85	0.38	23.30	0.43	0.56	1366.67.....	488.10	22.08	0.08	21.58	0.09	0.50
1226.08.....	230.57	24.20	0.47	22.44	0.18	1.76	1368.02.....	199.62	20.52	0.02	19.75	0.01	0.76
1226.28.....	479.12	22.53	0.09	21.16	0.05	1.38	1369.11.....	504.07	19.76	0.03	19.96	0.03	-0.20
1229.38.....	615.15	22.87	0.16	22.06	0.12	0.80	1372.36.....	426.11	21.54	0.05	20.29	0.03	1.25
1229.96.....	319.60	22.29	0.09	21.41	0.06	0.88	1376.12.....	546.94	21.80	0.05	21.31	0.07	0.48
1231.03.....	345.36	23.96	0.33	23.67	0.43	0.29	1376.72.....	449.13	23.10	0.24	21.31	0.05	1.79
1235.07.....	513.31	23.89	0.30	23.22	0.43	0.67	1377.96.....	592.86	23.08	0.17	21.52	0.08	1.55
1239.74.....	627.15	23.07	0.17	21.64	0.09	1.43	1378.21.....	540.29	20.76	0.03	20.76	0.06	0.00
1247.31.....	261.34	21.82	0.06	21.83	0.12	-0.01	1379.96.....	363.86	23.86	0.39	22.80	0.28	1.06
1247.62.....	516.54	23.85	0.36	22.23	0.14	1.63	1382.19.....	576.75	20.58	0.02	20.53	0.05	0.05
1247.64.....	351.17	23.80	0.30	22.79	0.25	1.01	1385.16.....	413.52	22.53	0.12	21.68	0.08	0.84
1253.48.....	556.40	21.11	0.03	20.51	0.04	0.60	1386.40.....	321.56	22.28	0.07	22.15	0.14	0.13
1254.62.....	300.28	22.61	0.12	22.63	0.22	-0.02	1386.49.....	586.57	21.39	0.04	21.92	0.10	-0.53
1254.71.....	334.65	22.86	0.13	21.81	0.08	1.06	1386.51.....	547.41	22.39	0.11	23.19	0.43	-0.81
1255.75.....	504.02	23.69	0.30	22.07	0.14	1.62	1386.84.....	522.92	23.08	0.21	21.58	0.08	1.50
1259.59.....	320.79	21.66	0.05	21.98	0.14	-0.32	1388.59.....	606.20	22.96	0.20	22.33	0.15	0.64
1260.12.....	505.51	21.33	0.03	21.44	0.07	-0.12	1389.25.....	648.62	23.40	0.24	21.77	0.10	1.63
1261.71.....	146.11	17.83	0.00	16.78	0.00	1.05	1394.07.....	116.20	22.21	0.08	21.48	0.09	0.73
1262.23.....	427.45	23.89	0.34	22.52	0.18	1.38	1395.98.....	552.49	20.47	0.03	20.49	0.04	-0.01
1263.91.....	491.22	20.80	0.03	19.29	0.01	1.51	1397.66.....	412.18	23.51	0.25	21.61	0.08	1.91
1268.90.....	612.41	23.56	0.27	22.39	0.14	1.17	1399.49.....	542.57	22.77	0.14	21.00	0.06	1.76
1273.44.....	252.86	23.57	0.29	23.17	0.38	0.40	1399.64.....	579.27	21.02	0.03	20.84	0.05	0.18
1278.94.....	452.42	23.20	0.21	22.15	0.13	1.05	1406.38.....	535.16	21.78	0.06	22.16	0.15	-0.38
1281.66.....	553.17	22.85	0.13	21.98	0.12	0.87	1407.48.....	473.06	20.99	0.03	21.21	0.06	-0.22
1283.75.....	630.51	22.83	0.13	21.86	0.10	0.96	1407.87.....	569.76	21.33	0.04	19.39	0.01	1.95
1292.02.....	612.76	22.60	0.13	21.76	0.09	0.84	1409.11.....	451.51	20.00	0.01	18.22	0.01	1.78
1292.49.....	338.51	21.89	0.05	20.63	0.04	1.26	1409.41.....	477.50	20.90	0.03	21.41	0.06	-0.51
1293.61.....	554.10	20.07	0.01	18.53	0.01	1.54	1409.73.....	504.57	22.27	0.09	21.32	0.06	0.95
1293.78.....	645.11	23.08	0.18	22.31	0.36	0.77	1413.23.....	429.83	22.63	0.13	21.47	0.07	1.16
1295.09.....	618.43	22.21	0.09	21.94	0.14	0.27	1414.53.....	465.01	21.99	0.08	21.96	0.11	0.03
1297.94.....	507.24	20.98	0.08	21.45	0.09	-0.48	1416.10.....	620.47	21.61	0.05	20.41	0.03	1.20
1299.77.....	521.89	22.26	0.13	22.62	0.22	-0.36	1416.66.....	449.69	22.70	0.14	22.74	0.21	-0.04
1301.39.....	495.49	22.72	0.16	22.61	0.20	0.10	1418.23.....	532.64	23.72	0.39	22.89	0.29	0.83
1301.84.....	506.78	21.23	0.11	21.51	0.08	-0.28	1418.35.....	602.06	23.18	0.22	22.86	0.29	0.32
1302.74.....	237.53	21.70	0.05	21.37	0.06	0.33	1422.73.....	612.17	21.51	0.04	20.85	0.05	0.66
1308.38.....	579.52	22.59	0.13	21.98	0.12	0.62	1423.70.....	284.34	22.75	0.15	21.79	0.10	0.97
1308.51.....	500.39	21.71	0.08	22.17	0.17	-0.45	1424.18.....	539.87	24.22	0.49	21.94	0.13	2.28
1308.92.....	193.84	21.90	0.06	21.86	0.10	0.04	1424.52.....	454.57	23.40	0.23	22.18	0.15	1.22
1312.48.....	585.86	22.03	0.07	22.18	0.16	-0.15	1424.66.....	618.28	21.80	0.05	20.75	0.04	1.05
1313.47.....	663.85	22.37	0.08	20.81	0.04	1.56	1426.39.....	439.47	22.06	0.10	23.35	0.52	-1.29
1314.00.....	265.23	21.11	0.03	21.48	0.07	-0.37	1428.91.....	576.78	23.92	0.48	21.89	0.11	2.03
1317.29.....	227.35	20.92	0.02	19.30	0.01	1.62	1429.35.....	480.43	21.09	0.04	19.78	0.02	1.31
1317.85.....	466.60	23.54	0.28	22.75	0.28	0.78	1429.51.....	528.12	22.20	0.10	21.00	0.05	1.21
1322.90.....	561.67	20.62	0.02	18.91	0.01	1.72	1429.92.....	565.37	23.02	0.16	22.02	0.14	1.00
1327.33.....	360.35	23.52	0.24	22.80	0.22	0.73	1430.03.....	317.72	23.01	0.16	21.73	0.09	1.28
1327.54.....	490.28	22.82	0.15	22.10	0.14	0.72	1430.89.....	590.26	22.22	0.09	20.97	0.05	1.25
1327.94.....	532.99	23.34	0.21	21.74	0.09	1.60	1431.07.....	100.77	24.09	0.39	22.44	0.21	1.65
1329.80.....	457.31	20.53	0.02	20.73	0.03	-0.20	1431.66.....	545.29	22.06	0.08	21.13	0.06	0.94
1330.47.....	582.96	22.60	0.15	21.87	0.11	0.73	1433.15.....	423.54	21.17	0.04	19.75	0.03	1.43
1331.10.....	389.03	21.11	0.04	21.75	0.09	-0.64	1433.58.....	576.85	22.95	0.16	22.29	0.19	0.66
1332.79.....	396.99	22.41	0.09	22.63	0.22	-0.23	1436.19.....	652.20	21.35	0.04	21.49	0.09	-0.14
1335.57.....	487.26	23.27	0.23	21.91	0.12	1.37	1437.00.....	456.81	21.44	0.05	20.41	0.04	1.03
1338.68.....	550.17	22.10	0.08	19.88	0.02	2.22	1438.90.....	585.88	23.04	0.18	22.06	0.14	0.98
1340.76.....	532.52	22.66	0.13	22.51	0.19	0.15	1439.30.....	431.96	21.24	0.05	21.51	0.09	-0.27
1341.32.....	376.16	22.18	0.09	21.62	0.09	0.56	1439.93.....	634.17	23.33	0.25	21.69	0.11	1.64
1343.29.....	606.80	24.02	0.50	22.27	0.17	1.76	1440.60.....	338.44	21.91	0.07	22.04	0.14	-0.13
1343.48.....	392.84	20.77	0.05	21.21	0.06	-0.44	1441.53.....	220.43	23.95	0.46	21.87	0.09	2.09
1344.63.....	420.05	22.64	0.12	23.02	0.28	-0.39	1442.07.....	501.87	21.52	0.06	20.41	0.04	1.11

TABLE 2—Continued

X (1)	Y (2)	V (3)	σ_V (4)	I (5)	σ_I (6)	$V - I$ (7)	X (1)	Y (2)	V (3)	σ_V (4)	I (5)	σ_I (6)	$V - I$ (7)
1443.16.....	486.49	23.21	0.18	22.43	0.18	0.77	1509.95.....	592.72	22.46	0.18	21.12	0.07	1.34
1444.16.....	474.48	22.05	0.07	21.83	0.11	0.21	1512.07.....	654.91	23.31	0.28	22.30	0.16	1.01
1444.24.....	608.35	23.98	0.38	22.78	0.23	1.19	1513.03.....	540.19	21.68	0.07	21.57	0.09	0.12
1444.96.....	629.56	23.75	0.30	22.00	0.12	1.76	1513.05.....	522.82	20.27	0.02	20.64	0.03	-0.37
1449.93.....	441.43	22.39	0.11	22.26	0.14	0.13	1513.22.....	504.59	21.15	0.04	21.12	0.06	0.04
1450.87.....	557.13	23.74	0.38	21.92	0.12	1.82	1513.29.....	439.18	20.78	0.02	18.95	0.01	1.83
1451.41.....	460.05	21.55	0.05	20.88	0.05	0.67	1513.45.....	574.20	20.87	0.03	20.17	0.02	0.70
1452.09.....	509.79	23.41	0.29	21.70	0.10	1.71	1513.54.....	622.13	22.67	0.16	21.93	0.12	0.74
1452.15.....	568.30	20.72	0.07	21.11	0.09	-0.40	1513.72.....	559.31	21.55	0.05	20.40	0.03	1.15
1453.08.....	564.59	21.31	0.07	21.47	0.12	-0.15	1515.85.....	353.85	23.63	0.35	22.28	0.17	1.35
1453.30.....	585.40	22.71	0.13	21.95	0.12	0.76	1516.32.....	602.72	22.33	0.12	21.57	0.08	0.76
1454.49.....	467.31	21.37	0.06	20.91	0.06	0.46	1517.92.....	567.95	20.33	0.02	20.72	0.04	-0.39
1455.43.....	615.92	23.17	0.20	21.77	0.08	1.39	1518.10.....	619.55	22.76	0.17	21.97	0.14	0.80
1455.68.....	340.80	21.81	0.05	20.71	0.03	1.10	1520.05.....	527.86	22.02	0.08	21.36	0.07	0.66
1456.82.....	478.48	22.17	0.08	21.14	0.06	1.04	1520.99.....	380.90	20.81	0.04	19.59	0.02	1.22
1456.92.....	512.68	22.41	0.13	21.95	0.11	0.46	1522.43.....	583.62	20.73	0.04	19.39	0.02	1.33
1457.65.....	625.79	23.66	0.28	22.07	0.16	1.58	1522.82.....	600.36	22.35	0.13	21.31	0.07	1.04
1457.76.....	572.82	21.41	0.07	21.86	0.11	-0.45	1523.97.....	589.16	20.84	0.04	19.55	0.02	1.29
1458.23.....	461.08	21.40	0.03	21.54	0.08	-0.14	1524.23.....	468.05	22.65	0.16	22.47	0.18	0.18
1458.58.....	591.35	20.65	0.02	20.88	0.05	-0.24	1525.14.....	452.23	23.27	0.25	21.88	0.09	1.39
1458.84.....	526.12	21.68	0.07	21.40	0.08	0.28	1525.46.....	433.07	21.19	0.04	21.77	0.10	-0.59
1459.38.....	424.86	22.40	0.09	22.04	0.12	0.36	1525.71.....	342.81	21.82	0.06	22.01	0.10	-0.19
1460.39.....	565.26	21.12	0.07	21.77	0.12	-0.65	1526.46.....	298.60	24.11	0.42	22.40	0.20	1.71
1463.77.....	587.20	22.97	0.18	21.48	0.08	1.49	1527.19.....	476.67	23.08	0.16	23.25	0.43	-0.17
1464.02.....	471.59	22.01	0.06	21.57	0.08	0.44	1527.26.....	507.16	23.08	0.20	21.77	0.11	1.32
1464.81.....	373.69	23.01	0.17	22.01	0.13	1.00	1527.42.....	103.43	22.04	0.07	21.33	0.07	0.71
1465.57.....	315.54	22.77	0.14	21.00	0.07	1.77	1527.45.....	654.78	22.97	0.16	22.95	0.29	0.02
1465.80.....	582.19	22.30	0.11	23.26	0.38	-0.96	1530.85.....	637.47	22.07	0.10	22.24	0.17	-0.18
1467.88.....	564.29	22.60	0.13	23.15	0.38	-0.54	1531.86.....	327.75	22.74	0.12	21.47	0.07	1.26
1468.09.....	425.38	23.92	0.44	22.90	0.24	1.02	1532.44.....	600.76	20.85	0.03	21.69	0.11	-0.84
1468.34.....	515.15	21.70	0.07	20.48	0.03	1.22	1532.44.....	556.84	19.90	0.02	20.03	0.03	-0.13
1469.55.....	459.70	22.13	0.09	21.35	0.08	0.78	1533.51.....	651.45	23.08	0.18	22.31	0.17	0.76
1470.14.....	388.94	21.84	0.05	20.73	0.04	1.10	1533.62.....	520.26	22.58	0.11	21.17	0.06	1.41
1470.50.....	593.74	20.82	0.04	21.13	0.05	-0.31	1533.63.....	536.89	21.84	0.09	21.30	0.10	0.55
1471.74.....	501.92	21.15	0.05	21.21	0.08	-0.06	1533.70.....	351.19	21.23	0.04	19.95	0.02	1.28
1473.98.....	559.52	22.55	0.14	22.46	0.21	0.09	1534.97.....	250.15	24.05	0.49	22.81	0.36	1.24
1474.31.....	468.67	22.69	0.15	23.18	0.41	-0.49	1535.93.....	388.85	22.52	0.12	21.85	0.08	0.67
1479.60.....	481.52	22.75	0.14	21.56	0.10	1.20	1536.09.....	560.72	21.50	0.05	20.52	0.05	0.98
1479.74.....	544.11	20.79	0.03	19.19	0.02	1.59	1536.29.....	440.23	21.27	0.03	21.15	0.07	0.12
1480.43.....	646.13	23.56	0.28	23.13	0.33	0.43	1536.71.....	196.99	23.73	0.33	22.70	0.22	1.03
1482.35.....	552.31	22.17	0.09	21.63	0.09	0.54	1537.00.....	396.15	22.19	0.10	21.02	0.05	1.17
1482.80.....	510.07	21.10	0.03	21.62	0.06	-0.52	1537.27.....	530.37	22.31	0.11	20.99	0.05	1.33
1483.71.....	606.17	21.94	0.08	20.36	0.04	1.58	1537.83.....	461.99	19.50	0.02	19.74	0.02	-0.24
1484.69.....	461.55	22.39	0.11	21.45	0.07	0.94	1538.07.....	521.18	22.40	0.10	22.07	0.15	0.33
1485.02.....	525.32	21.94	0.07	20.39	0.03	1.55	1538.81.....	274.53	23.76	0.34	22.78	0.25	0.98
1486.38.....	448.12	21.94	0.07	20.95	0.05	0.99	1539.76.....	485.97	23.60	0.28	22.61	0.18	0.99
1486.91.....	508.80	22.08	0.07	22.46	0.18	-0.38	1540.32.....	588.02	20.48	0.03	19.25	0.01	1.22
1487.28.....	467.53	23.74	0.34	21.75	0.07	1.99	1541.41.....	559.19	21.81	0.08	20.73	0.04	1.08
1487.61.....	561.43	22.74	0.18	21.31	0.08	1.44	1541.70.....	625.85	21.42	0.10	20.36	0.05	1.06
1488.12.....	332.34	21.33	0.04	19.87	0.02	1.46	1545.10.....	249.33	23.04	0.16	22.19	0.12	0.85
1488.13.....	307.07	22.72	0.13	21.73	0.10	1.00	1545.20.....	562.64	21.35	0.05	20.64	0.05	0.71
1491.39.....	529.13	21.64	0.05	21.39	0.08	0.26	1545.36.....	499.45	23.15	0.22	21.56	0.08	1.59
1491.79.....	306.07	23.83	0.36	23.18	0.40	0.65	1546.44.....	386.76	22.70	0.14	21.53	0.08	1.17
1492.46.....	597.67	21.87	0.06	20.73	0.04	1.14	1547.31.....	364.45	20.06	0.01	20.40	0.03	-0.34
1493.25.....	492.37	22.42	0.10	21.58	0.07	0.85	1548.01.....	575.77	21.34	0.07	20.46	0.03	0.88
1494.08.....	569.02	20.83	0.03	21.39	0.07	-0.56	1549.45.....	447.65	23.95	0.38	21.01	0.06	2.94
1494.48.....	575.44	22.23	0.10	21.60	0.09	0.63	1549.59.....	531.88	22.20	0.10	21.16	0.05	1.04
1495.59.....	537.26	19.19	0.01	19.35	0.01	-0.16	1549.81.....	615.46	19.99	0.02	18.28	0.01	1.72
1497.41.....	483.03	21.36	0.05	21.41	0.08	-0.05	1550.10.....	518.12	22.07	0.08	22.30	0.15	-0.22
1498.41.....	506.89	21.28	0.06	20.03	0.02	1.25	1552.54.....	655.25	21.56	0.09	21.02	0.05	0.54
1498.80.....	633.88	22.61	0.17	21.51	0.09	1.10	1552.59.....	575.29	20.69	0.04	20.89	0.05	-0.20
1500.95.....	402.88	20.85	0.03	19.05	0.01	1.80	1552.80.....	266.37	23.13	0.22	21.20	0.05	1.93
1501.03.....	587.38	22.49	0.09	20.59	0.04	1.91	1556.17.....	370.36	21.60	0.05	21.99	0.14	-0.40
1501.45.....	619.68	22.49	0.10	21.99	0.11	0.50	1556.33.....	363.94	22.26	0.11	21.82	0.14	0.44
1501.51.....	640.76	21.53	0.05	21.50	0.09	0.03	1556.69.....	572.72	21.51	0.08	20.94	0.06	0.57
1503.09.....	559.14	22.25	0.12	20.83	0.04	1.42	1557.25.....	384.33	22.01	0.08	22.50	0.21	-0.50
1503.70.....	604.17	23.64	0.33	22.71	0.29	0.93	1558.64.....	601.44	22.35	0.10	21.07	0.05	1.27
1503.85.....	581.22	21.35	0.04	21.27	0.08	0.08	1558.70.....	397.71	23.65	0.36	21.75	0.11	1.90
1504.47.....	576.76	20.73	0.03	20.90	0.07	-0.17	1562.00.....	333.64	23.38	0.28	22.76	0.28	0.62
1505.05.....	476.60	21.46	0.05	21.53	0.10	-0.07	1562.43.....	449.13	22.12	0.09	21.10	0.05	1.03
1506.97.....	351.73	21.95	0.05	22.16	0.13	-0.21	1563.17.....	606.46	23.08	0.20	21.22	0.05	1.86
1507.30.....	610.18	20.55	0.03	20.76	0.05	-0.22	1566.89.....	514.48	23.15	0.28	22.81	0.32	0.34
1507.42.....	630.99	22.34	0.11	22.09	0.17	0.25	1566.91.....	377.24	18.79	0.01	17.77	0.01	1.01

TABLE 2—Continued

X (1)	Y (2)	V (3)	σ_V (4)	I (5)	σ_I (6)	$V - I$ (7)	X (1)	Y (2)	V (3)	σ_V (4)	I (5)	σ_I (6)	$V - I$ (7)
1567.21.....	307.70	21.80	0.07	20.68	0.03	1.12	1618.10.....	413.48	20.52	0.02	20.72	0.04	-0.21
1567.43.....	535.59	19.09	0.02	19.00	0.02	0.09	1618.88.....	640.99	22.24	0.10	22.24	0.14	0.01
1567.83.....	612.05	22.93	0.18	21.46	0.07	1.47	1618.91.....	569.03	22.14	0.08	22.23	0.19	-0.09
1568.40.....	402.70	20.21	0.02	20.11	0.02	0.09	1618.98.....	612.63	22.89	0.18	21.60	0.11	1.29
1569.59.....	555.76	20.98	0.05	21.63	0.11	-0.65	1619.29.....	420.51	21.80	0.07	22.09	0.12	-0.29
1570.30.....	582.62	23.99	0.38	22.85	0.24	1.14	1619.33.....	365.93	22.88	0.14	22.57	0.20	0.30
1570.87.....	608.71	22.54	0.12	21.47	0.09	1.07	1619.33.....	501.62	23.21	0.19	18.64	0.13	4.57
1573.07.....	145.02	24.12	0.45	23.21	0.31	0.91	1619.85.....	525.60	20.49	0.03	20.92	0.06	-0.43
1573.11.....	525.97	21.33	0.07	20.14	0.03	1.19	1620.04.....	358.58	23.60	0.36	21.93	0.11	1.67
1575.67.....	447.51	21.26	0.06	20.91	0.05	0.35	1620.06.....	515.55	20.94	0.03	19.46	0.02	1.48
1575.79.....	359.57	21.90	0.06	22.60	0.22	-0.70	1622.35.....	657.77	22.68	0.15	21.93	0.12	0.76
1575.86.....	559.40	21.29	0.06	22.61	0.24	-1.32	1623.34.....	503.97	22.60	0.13	21.07	0.07	1.53
1576.13.....	612.99	22.40	0.12	21.56	0.08	0.84	1623.70.....	538.16	21.02	0.04	19.96	0.02	1.06
1576.35.....	629.50	22.74	0.17	22.78	0.30	-0.05	1624.02.....	628.90	21.20	0.03	22.05	0.19	-0.84
1576.78.....	427.21	23.85	0.41	22.67	0.21	1.18	1625.04.....	400.34	21.44	0.05	21.87	0.10	-0.43
1577.09.....	553.87	20.92	0.06	21.90	0.12	-0.98	1625.29.....	472.84	21.89	0.07	20.55	0.04	1.34
1577.75.....	647.70	22.10	0.10	22.11	0.14	0.00	1625.76.....	311.68	21.07	0.04	19.86	0.03	1.21
1579.53.....	450.69	21.91	0.06	21.97	0.12	-0.06	1626.49.....	548.62	22.64	0.14	20.38	0.04	2.26
1579.55.....	497.26	22.37	0.10	21.32	0.06	1.05	1626.74.....	426.13	21.87	0.07	20.38	0.03	1.49
1581.43.....	619.18	22.51	0.15	22.58	0.18	-0.07	1626.77.....	448.50	21.44	0.05	21.25	0.06	0.20
1581.92.....	345.89	22.34	0.10	21.16	0.07	1.18	1626.82.....	622.56	22.54	0.13	20.72	0.05	1.81
1582.03.....	612.74	21.76	0.06	21.99	0.12	-0.23	1627.65.....	583.32	18.28	0.01	18.29	0.01	-0.01
1582.28.....	330.64	21.16	0.03	21.56	0.08	-0.40	1627.79.....	490.46	23.78	0.39	21.99	0.12	1.80
1582.34.....	636.22	23.66	0.39	21.35	0.07	2.31	1631.80.....	319.54	17.64	0.01	16.84	0.01	0.80
1582.84.....	406.49	22.62	0.15	21.96	0.11	0.66	1632.15.....	459.23	22.44	0.13	21.34	0.07	1.09
1583.35.....	377.23	18.74	0.01	17.52	0.01	1.22	1632.35.....	659.54	23.16	0.27	21.70	0.13	1.46
1584.80.....	663.21	22.32	0.10	21.69	0.09	0.62	1633.76.....	598.94	21.06	0.04	21.33	0.06	-0.28
1585.60.....	577.96	20.96	0.03	19.43	0.01	1.53	1633.95.....	200.21	23.92	0.43	23.12	0.35	0.80
1585.72.....	278.22	23.10	0.18	22.56	0.22	0.54	1635.44.....	502.43	20.85	0.03	18.90	0.01	1.95
1586.75.....	202.28	23.93	0.37	23.03	0.34	0.90	1637.29.....	561.73	20.82	0.03	20.83	0.04	0.00
1587.68.....	545.85	23.85	0.45	23.25	0.46	0.60	1637.64.....	548.45	21.53	0.05	22.84	0.34	-1.31
1588.63.....	520.26	20.09	0.02	20.60	0.03	-0.51	1637.76.....	635.98	22.35	0.12	21.43	0.09	0.92
1589.07.....	431.30	21.97	0.12	22.10	0.14	-0.13	1638.37.....	450.93	20.85	0.03	20.74	0.04	0.11
1589.15.....	612.32	22.54	0.12	21.68	0.14	0.86	1638.94.....	444.23	22.08	0.09	21.76	0.09	0.32
1590.49.....	482.68	23.37	0.27	21.59	0.09	1.78	1640.83.....	570.70	23.05	0.24	21.35	0.10	1.70
1591.98.....	663.64	20.61	0.03	21.00	0.07	-0.39	1640.98.....	479.22	21.91	0.07	21.77	0.09	0.14
1592.01.....	637.43	20.46	0.02	20.36	0.04	0.10	1641.22.....	521.45	22.94	0.20	22.54	0.22	0.40
1593.98.....	531.43	21.26	0.05	21.21	0.07	0.05	1641.81.....	509.58	22.65	0.13	21.49	0.07	1.16
1594.51.....	420.43	21.69	0.05	21.76	0.09	-0.06	1642.19.....	610.97	20.16	0.05	19.12	0.03	1.04
1594.54.....	470.30	22.90	0.18	22.38	0.18	0.53	1642.53.....	544.93	21.81	0.06	20.79	0.04	1.02
1594.80.....	425.30	22.03	0.10	21.27	0.07	0.75	1645.73.....	663.45	20.77	0.03	19.44	0.02	1.33
1595.05.....	619.38	22.32	0.09	21.74	0.12	0.58	1648.02.....	574.60	23.03	0.20	22.26	0.15	0.77
1595.06.....	373.15	21.05	0.02	19.53	0.01	1.52	1648.89.....	629.68	22.48	0.12	21.16	0.08	1.32
1596.53.....	560.55	21.79	0.07	21.60	0.10	0.19	1650.31.....	542.19	22.22	0.12	20.42	0.04	1.80
1599.56.....	453.86	23.22	0.21	22.06	0.13	1.15	1652.04.....	505.71	22.25	0.10	21.02	0.05	1.23
1599.87.....	509.28	21.76	0.06	20.45	0.04	1.31	1653.38.....	526.92	22.45	0.13	21.45	0.09	1.00
1600.01.....	400.45	21.61	0.07	21.10	0.05	0.51	1653.55.....	628.22	22.22	0.10	21.00	0.06	1.22
1600.37.....	377.27	20.97	0.04	21.17	0.06	-0.20	1654.17.....	581.97	21.98	0.13	21.23	0.09	0.75
1602.76.....	351.07	22.62	0.12	22.39	0.19	0.22	1654.24.....	385.97	22.70	0.15	22.32	0.17	0.38
1603.26.....	364.07	23.09	0.19	21.97	0.12	1.12	1654.64.....	413.47	23.84	0.42	21.87	0.12	1.98
1603.62.....	220.94	23.98	0.44	22.35	0.16	1.63	1656.38.....	541.01	21.81	0.10	20.81	0.07	1.00
1603.64.....	592.04	22.82	0.14	21.00	0.06	1.82	1656.92.....	346.66	22.97	0.15	22.56	0.20	0.42
1603.86.....	597.08	22.81	0.17	21.25	0.08	1.56	1657.44.....	649.40	22.38	0.10	22.22	0.18	0.15
1604.26.....	537.99	21.22	0.04	19.70	0.02	1.53	1657.98.....	438.44	22.68	0.14	22.53	0.21	0.15
1604.84.....	641.89	22.21	0.10	21.59	0.08	0.62	1658.05.....	554.95	19.36	0.01	19.59	0.02	-0.23
1606.20.....	269.23	22.78	0.13	22.85	0.23	-0.07	1658.61.....	594.12	22.12	0.09	21.90	0.10	0.23
1606.54.....	389.72	24.22	0.51	22.83	0.26	1.39	1660.90.....	662.05	21.82	0.07	22.32	0.18	-0.50
1606.88.....	296.33	22.98	0.17	21.56	0.07	1.42	1660.90.....	549.56	20.23	0.03	20.17	0.05	0.06
1607.71.....	620.31	22.81	0.24	22.04	0.12	0.77	1662.66.....	647.53	21.57	0.06	21.64	0.11	-0.07
1609.57.....	499.15	21.91	0.09	21.97	0.13	-0.07	1663.27.....	620.04	22.30	0.12	21.67	0.11	0.63
1611.11.....	614.26	22.21	0.09	22.84	0.25	-0.63	1663.66.....	589.66	21.20	0.06	20.12	0.04	1.08
1611.68.....	510.12	23.79	0.33	22.36	0.19	1.43	1664.07.....	536.82	22.26	0.11	22.43	0.19	-0.17
1611.96.....	551.92	21.84	0.10	20.78	0.06	1.06	1664.83.....	493.59	20.74	0.03	21.16	0.06	-0.42
1612.09.....	453.03	22.02	0.09	21.65	0.11	0.38	1665.10.....	637.64	20.79	0.03	21.25	0.06	-0.47
1612.16.....	290.34	23.27	0.28	23.56	0.53	-0.29	1665.50.....	545.39	22.57	0.15	21.50	0.11	1.06
1612.49.....	531.53	21.86	0.10	22.50	0.29	-0.64	1667.62.....	360.90	22.48	0.11	21.68	0.09	0.80
1615.35.....	445.72	21.68	0.06	21.51	0.08	0.17	1667.83.....	465.83	23.19	0.16	21.90	0.09	1.28
1615.37.....	582.79	21.67	0.10	21.94	0.12	-0.27	1668.28.....	554.67	20.24	0.05	19.88	0.02	0.35
1615.62.....	556.55	22.02	0.11	21.50	0.09	0.52	1669.36.....	444.50	23.25	0.20	21.50	0.07	1.75
1616.15.....	338.26	21.75	0.05	22.18	0.13	-0.43	1671.24.....	584.83	22.48	0.34	21.63	0.13	0.85
1617.11.....	401.68	22.79	0.14	21.64	0.10	1.16	1671.31.....	463.08	23.33	0.26	22.18	0.15	1.15
1617.19.....	473.39	22.96	0.16	22.14	0.12	0.82	1671.34.....	599.72	22.05	0.10	22.52	0.28	-0.47
1617.43.....	542.29	20.94	0.03	21.34	0.09	-0.40	1671.49.....	605.58	22.01	0.11	21.84	0.14	0.17

TABLE 2—Continued

<i>X</i> (1)	<i>Y</i> (2)	<i>V</i> (3)	σ_V (4)	<i>I</i> (5)	σ_I (6)	<i>V</i> − <i>I</i> (7)	<i>X</i> (1)	<i>Y</i> (2)	<i>V</i> (3)	σ_V (4)	<i>I</i> (5)	σ_I (6)	<i>V</i> − <i>I</i> (7)
1672.06.....	460.73	23.59	0.34	22.72	0.26	0.88	1711.52.....	620.80	21.81	0.11	21.48	0.09	0.33
1672.07.....	454.25	23.22	0.19	22.37	0.16	0.85	1711.60.....	373.71	22.24	0.08	21.44	0.08	0.80
1672.46.....	503.02	23.83	0.39	21.81	0.12	2.02	1712.71.....	553.22	20.38	0.02	20.58	0.04	−0.20
1672.58.....	479.35	21.02	0.04	19.72	0.02	1.30	1712.82.....	575.47	21.82	0.09	21.41	0.08	0.41
1674.47.....	663.75	21.69	0.09	20.59	0.05	1.10	1712.87.....	636.74	22.29	0.14	21.30	0.09	0.99
1676.80.....	594.43	21.83	0.10	22.10	0.17	−0.27	1712.88.....	561.48	22.03	0.11	20.51	0.04	1.52
1676.99.....	485.72	20.98	0.03	19.63	0.02	1.35	1713.10.....	605.28	20.72	0.08	19.90	0.08	0.82
1679.03.....	416.12	23.01	0.21	21.53	0.08	1.48	1713.14.....	628.97	21.22	0.04	21.38	0.07	−0.17
1679.87.....	487.75	20.77	0.03	19.43	0.02	1.34	1713.29.....	172.81	18.81	0.01	17.50	0.01	1.31
1680.75.....	315.23	23.23	0.21	21.71	0.08	1.52	1714.41.....	527.65	21.78	0.09	21.48	0.10	0.31
1680.97.....	584.76	22.88	0.19	22.69	0.22	0.19	1714.97.....	363.62	23.65	0.36	23.36	0.47	0.29
1681.97.....	515.65	21.59	0.05	22.82	0.30	−1.23	1715.43.....	447.52	23.13	0.22	21.95	0.14	1.18
1683.01.....	571.77	21.78	0.06	21.66	0.08	0.12	1715.46.....	326.92	23.85	0.38	22.80	0.24	1.04
1684.15.....	435.40	22.03	0.09	21.23	0.06	0.80	1716.40.....	424.20	21.99	0.11	21.50	0.09	0.49
1684.20.....	507.46	20.79	0.02	19.61	0.03	1.18	1718.97.....	539.17	20.73	0.07	20.65	0.07	0.08
1686.47.....	602.18	20.47	0.07	20.83	0.08	−0.36	1719.00.....	501.54	22.93	0.16	21.16	0.06	1.77
1686.70.....	331.71	22.23	0.08	21.19	0.06	1.03	1720.57.....	653.66	23.04	0.18	21.84	0.13	1.20
1686.78.....	491.88	21.30	0.05	20.08	0.03	1.22	1720.79.....	590.41	20.52	0.10	15.87	0.05	4.65
1687.74.....	618.46	21.43	0.08	20.47	0.06	0.96	1721.85.....	551.24	22.74	0.16	22.33	0.19	0.41
1689.05.....	630.62	21.84	0.09	21.52	0.10	0.32	1722.53.....	637.60	22.53	0.19	22.16	0.14	0.37
1690.77.....	265.77	23.09	0.18	22.51	0.18	0.58	1722.96.....	380.43	21.47	0.04	20.89	0.06	0.58
1690.83.....	567.96	21.25	0.09	20.84	0.09	0.41	1723.18.....	516.24	20.28	0.05	19.05	0.01	1.22
1691.14.....	520.84	20.12	0.02	20.54	0.03	−0.42	1723.20.....	526.21	21.76	0.11	22.13	0.14	−0.36
1692.42.....	600.79	20.24	0.06	20.45	0.05	−0.20	1725.21.....	618.67	22.13	0.09	21.64	0.13	0.49
1694.00.....	657.57	21.41	0.05	20.24	0.04	1.17	1726.25.....	628.65	23.56	0.31	21.69	0.11	1.87
1695.82.....	481.95	23.25	0.26	20.79	0.05	2.46	1726.43.....	463.43	22.36	0.11	22.02	0.11	0.34
1696.00.....	436.79	21.64	0.07	22.42	0.19	−0.78	1726.56.....	651.02	22.42	0.09	21.33	0.07	1.09
1696.43.....	442.96	21.65	0.06	21.51	0.10	0.13	1726.92.....	595.16	20.15	0.08	19.09	0.04	1.06
1696.67.....	532.62	20.81	0.03	19.02	0.01	1.79	1728.26.....	486.56	21.97	0.08	21.06	0.07	0.92
1697.42.....	551.70	21.68	0.09	21.33	0.09	0.35	1728.86.....	530.03	21.34	0.04	21.09	0.07	0.25
1698.33.....	572.92	22.10	0.10	20.79	0.08	1.32	1729.28.....	624.73	21.71	0.08	21.11	0.08	0.60
1700.68.....	507.18	20.72	0.02	21.38	0.07	−0.67	1729.33.....	615.37	22.26	0.13	21.01	0.09	1.25
1700.71.....	475.52	23.03	0.23	22.47	0.17	0.56	1729.35.....	604.91	20.23	0.06	19.40	0.03	0.84
1700.91.....	521.83	21.26	0.04	20.03	0.02	1.23	1732.03.....	648.37	23.02	0.17	21.65	0.12	1.37
1701.43.....	637.32	22.52	0.15	21.67	0.10	0.85	1733.74.....	621.98	21.13	0.05	20.98	0.07	0.15
1702.78.....	664.11	21.77	0.09	21.02	0.08	0.74	1734.40.....	488.56	21.45	0.04	21.05	0.07	0.40
1703.80.....	575.51	21.44	0.05	20.17	0.04	1.27	1735.63.....	565.53	21.56	0.05	21.91	0.13	−0.35
1703.82.....	556.43	21.28	0.07	20.94	0.08	0.34	1736.58.....	593.56	20.34	0.06	19.50	0.04	0.84
1704.01.....	592.68	21.01	0.06	19.83	0.04	1.18	1738.37.....	343.45	23.11	0.17	22.26	0.14	0.85
1705.09.....	617.06	22.09	0.10	21.08	0.08	1.01	1738.92.....	270.54	23.49	0.30	22.19	0.16	1.30
1705.83.....	445.17	23.86	0.47	22.21	0.16	1.65	1739.06.....	643.63	22.16	0.13	21.80	0.14	0.35
1707.13.....	491.33	20.64	0.02	19.45	0.02	1.19	1740.36.....	422.98	23.09	0.22	22.93	0.28	0.16
1707.31.....	623.29	21.65	0.09	21.08	0.06	0.57	1740.64.....	242.81	20.86	0.03	18.73	0.02	2.13
1707.32.....	552.10	21.75	0.10	17.90	0.07	3.84	1741.08.....	639.64	22.09	0.07	21.53	0.11	0.57
1707.98.....	599.31	19.78	0.03	18.12	0.02	1.65	1741.81.....	259.60	23.67	0.41	23.56	0.46	0.11
1709.04.....	642.28	21.93	0.10	20.99	0.07	0.94	1742.73.....	533.22	23.40	0.30	23.57	0.54	−0.18
1709.19.....	570.80	21.03	0.04	21.26	0.08	−0.23	1745.49.....	511.50	23.42	0.28	22.75	0.27	0.67
1709.22.....	586.85	21.18	0.07	20.09	0.07	1.09	1746.27.....	325.36	22.42	0.11	22.40	0.19	0.02
1709.55.....	462.81	22.55	0.12	21.45	0.10	1.10	1746.56.....	414.51	23.28	0.21	21.39	0.15	1.89

grams for a total of 534 stars in the southeast portion of the IC 5152 disk, covering 6.7 arcmin². These are all the stars with centroids matched in *V* and *I* frames to better than 2.0 pixels (0''.6) and satisfying stringent criteria of photometric quality ($\sigma \leq 0.5$, $\chi \leq 2$, and sharpness ≥ -1). The sharpness criterion eliminates galaxies as well as possible star clusters. Contamination from foreground stars has not been subtracted from this diagram; this contamination is discussed in the next section.

In spite of the relatively small number of stars, a number of features can be identified in Figure 5. A tail of red giant stars is seen reaching *I* = 18.5 (we will argue below that this traces red supergiants rather than the red giant branch [RGB]). A blue main sequence with mean color *V*−*I* = 0.0 also reaches *I* = 18.5. A population of blue loop stars may also be seen, running in a sequence about 0.3 mag redder, parallel to the main sequence.

3.2. Reddening

Because of the high Galactic latitude, $b = -50^{\circ}19$, the foreground reddening toward IC 5152 is likely to be small. Based on the H I column density, Burstein & Heiles (1984) estimate the foreground reddening as $E(B-V) = 0.00$.

The bright foreground star HD 209142 gives an additional constraint on the reddening. Photometry from the ESA Tycho catalog (Hog et al. 1998) gives *V* = 7.78 and *B* = 8.01 for this A8V star. This is precisely the color expected for its type and indicates $E(B-V) < 0.02$. The star is at approximately 120 pc distance, which at this Galactic latitude is close to the edge of the absorbing gas layer in the Galactic disk. This result is consistent with the negligible reddening inferred by Burstein & Heiles (1984).

We can also estimate the foreground reddening by using the sharp blue cutoff in the stellar distribution of the outer

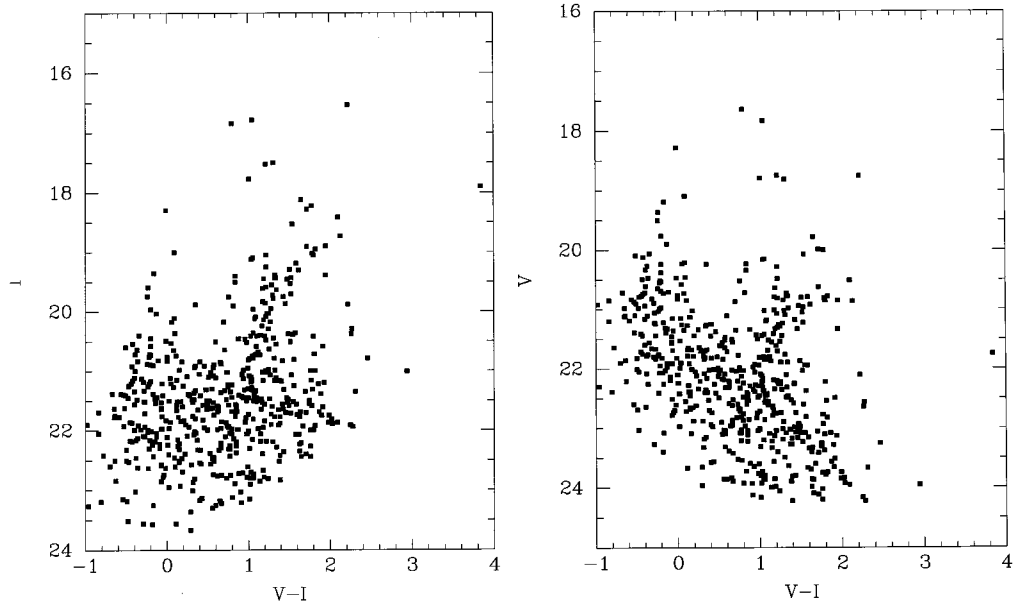


FIG. 5.—Color-magnitude diagrams for all the stars with V and I measured in IC 5152

IC 5152 fields. This cutoff is interpreted as the locus of the main sequence, which is nearly vertical in the theoretical color-magnitude diagrams, having an intrinsic color of $(V-I)_0 = -0.20$ (Bertelli et al. 1994). From the observed color we deduce $E(V-I) < 0.03$, consistent with the above-cited value. $E(B-V) < 0.02$ is equivalent to $E(V-I) < 0.03$ and $A_I < 0.03$, using the reddening ratios $E(V-I) = 1.60 E(B-V)$, $A_I = 1.49 E(B-V)$ of Rieke & Lebofsky (1985). We will adopt $E(V-I) = 0$ and $A_I = 0$.

The main sequence appears broadened more than expected from the photometric errors, from which we infer that there is substantial internal differential absorption in IC 5152. Webster et al. (1983) derive $c_{H\beta} = 0.23$ for one H II region, corresponding to $E(V-I) = 0.25$ and indicating the

presence of internal extinction near this H II region. Although internal extinction is (on average) less important for red giants than for luminous main-sequence stars, as the latter occur closer to the dusty star-forming regions, the effect also broadens the giant branches at fainter magnitudes.

3.3. Contamination from Foreground Stars and Background Galaxies

The foreground stars from the Milky Way halo and disk should appear as a plume of stars with $V-I = 0.7$, with total range covering about $0.4 \leq V-I \leq 1.5$. We divide the observed $9' \times 3'$ field in two zones, one containing the IC 5152 disk covering 6.7 arcmin^2 , and the rest containing

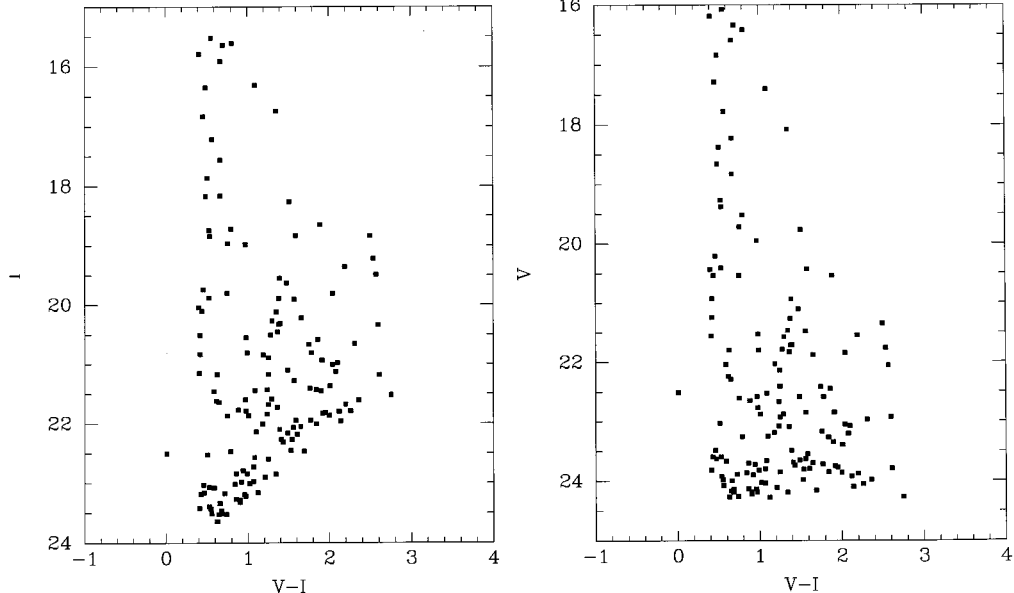


FIG. 6.—Color-magnitude diagrams of the background IC 5152 field

mostly foreground stars of our own galaxy and background galaxies, covering 16.5 arcmin². The photometry of $N = 144$ objects in the neighboring field is listed in Table 3, and their color-magnitude diagram is shown in Figure 6. The observed density of red stars ($V - I > 1.0$) in this region is one star arcmin⁻² with $I \leq 20$ and two stars arcmin⁻² with $I \leq 21$. Thus, in the location of the supergiant branch of IC 5152 of Figure 5, we expect no more than about 14 objects that may be nonmembers of this galaxy.

The few stars of Figure 6 located in the region corresponding to the IC 5152 supergiant branch may still be members of this galaxy if the IC 5152 disk is more extended than the region adopted above. From the Galactic model of Ratnatunga & Bahcall (1985), we expect 0.7 foreground halo stars arcmin⁻² with $V \leq 21$ and $0 \leq V - I \leq 2$ in this high-latitude field ($l = 343^{\circ}91$, $b = -50^{\circ}19$).

Since the galaxy/star ratio increases rapidly for faint magnitudes, the background galaxy contamination also has to be taken into account. Most of the brighter galaxies are resolved and are discarded by our sharpness criterion; only a few fainter and very compact ones may cause confusion. From Tyson (1988) we expect a galaxy density of 10^4 gal degree⁻² mag⁻¹ with $I < 21.5$. This would give ~ 75 galaxies in our 3×9 arcmin² field and only ~ 22 galaxies in the 6.7 arcmin² of IC 5152 corresponding to the color-magnitude diagram shown in Figure 5. However, the majority of these galaxies are resolved and were eliminated on that basis. In summary, the field contamination would not alter the appearance of Figure 5, which accurately represents the stellar content of the IC 5152 disk.

3.4. The Luminosity Function

An I -band luminosity function can be constructed by counting all the stars present in the I -frames, regardless of them matching the V -images. The normalized counts of $N = 770$ stars measured in the I -band are plotted in Figure 7. Two distinct breaks can be seen: the brightest at $I \approx 18.5 \pm 0.1$, and another break at $I = 20.4$. The luminosity function corresponding to the foreground stars and unresolved background galaxies is plotted in Figure 8 for comparison.

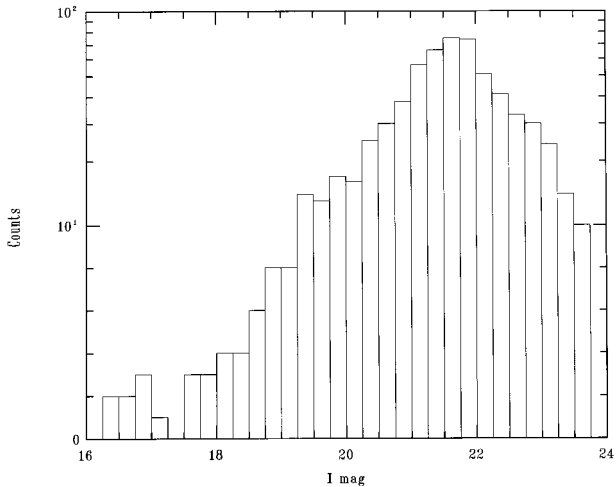


FIG. 7.— I -band luminosity function including all the stars with photometry in the 6.7 arcmin² field of the IC 5152 disk. The supergiant branch termination is seen at about $I = 18.5$ and the AGB termination at about $I = 21.0$.

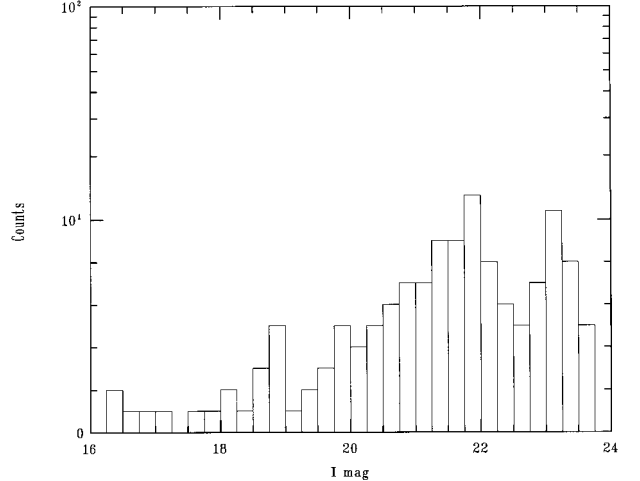


FIG. 8.— I -band luminosity function of the IC 5152 background field. This field covers 16.5 arcmin².

A bolometric luminosity function can be constructed for the red stars with $V - I > 0.8$ using the following relation:

$$M_{\text{bol}} = I_0 + 0.30 + 0.38(V - I)_0 - 0.14(V - I)^2 \\ - (m - M)_0$$

(Bessell & Wood 1984). The resulting bolometric luminosity function of the giant branches is shown in Figure 9. The two breaks are seen very clearly, at $m_{\text{bol}} = 16.5$ and $m_{\text{bol}} = 19$.

3.5. Interpretation

The sequence of red stars can contain red supergiants, asymptotic giant branch (AGB) stars, and RGB stars; the two breaks indicate at least two of these are present. Because the supergiant and/or the AGB break may not be obvious in a small system, a consistent interpretation could be possible at several distances. For a sparse color-magnitude diagram, further information is needed to remove the distance ambiguity (e.g., Tolstoy et al. 1998).

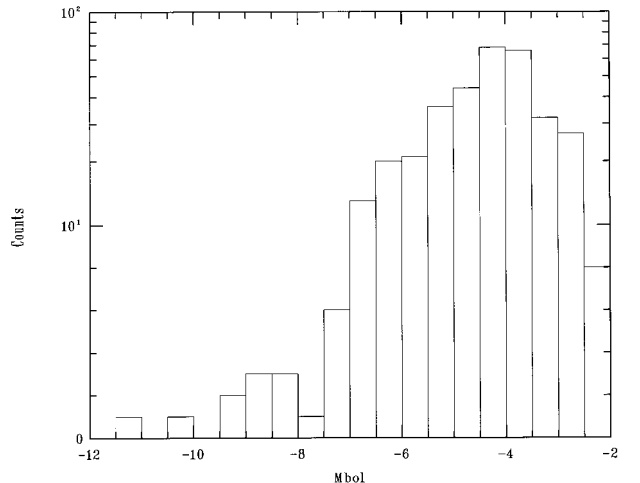


FIG. 9.—Bolometric luminosity function of IC 5152, including all the red stars with $V - I > 0.8$. The brightest red supergiants in this galaxy reach $M_{\text{bol}} = -10.5$, and the supergiant branch break is seen at $M_{\text{bol}} = -8$.

TABLE 3
PHOTOMETRY OF BACKGROUND FIELD

<i>X</i> (1)	<i>Y</i> (2)	<i>V</i> (3)	σ_V (4)	<i>I</i> (5)	σ_I (6)	<i>V</i> - <i>I</i> (7)	<i>X</i> (1)	<i>Y</i> (2)	<i>V</i> (3)	σ_V (4)	<i>I</i> (5)	σ_I (6)	<i>V</i> - <i>I</i> (7)
5.21	101.15	21.71	0.05	20.31	0.04	1.40	642.71	228.96	24.16	0.49	22.47	0.22	1.69
9.06	490.30	23.17	0.19	21.41	0.08	1.76	665.26	151.82	22.03	0.09	20.84	0.05	1.19
13.20	393.45	18.83	0.01	18.16	0.01	0.67	666.05	40.78	23.03	0.21	22.52	0.20	0.51
25.90	495.50	24.28	0.50	23.16	0.39	1.12	666.67	155.68	21.80	0.08	20.81	0.05	0.99
27.46	27.37	22.04	0.12	21.46	0.10	0.59	667.02	535.41	21.35	0.04	18.84	0.01	2.50
41.99	210.82	22.24	0.09	21.62	0.09	0.62	669.70	287.57	18.66	0.01	18.17	0.01	0.49
42.86	154.97	20.94	0.02	19.55	0.01	1.39	673.54	385.42	23.80	0.30	22.18	0.14	1.61
47.54	310.15	22.77	0.12	21.79	0.11	0.98	677.74	401.53	21.47	0.04	20.12	0.02	1.35
53.11	477.84	23.69	0.35	22.27	0.16	1.41	699.32	29.97	21.79	0.12	20.51	0.07	1.28
58.57	370.44	24.03	0.44	23.01	0.39	1.02	701.78	368.59	21.58	0.09	20.27	0.07	1.30
60.23	383.35	23.08	0.20	21.84	0.12	1.24	703.15	629.78	24.18	0.40	23.28	0.41	0.90
64.09	575.36	21.27	0.07	19.89	0.05	1.38	747.47	412.66	24.17	0.46	23.52	0.52	0.65
79.21	375.53	21.25	0.03	20.83	0.05	0.42	751.14	158.61	23.81	0.37	22.27	0.16	1.54
81.75	1.47	22.41	0.14	21.17	0.10	1.25	754.47	214.54	23.80	0.37	22.73	0.28	1.07
92.11	307.73	15.39	0.07	14.91	0.05	0.49	755.32	2.75	22.88	0.21	21.59	0.08	1.29
112.50.....	452.45	23.89	0.40	23.17	0.30	0.72	764.12	134.73	24.11	0.37	22.90	0.44	1.21
115.43.....	86.91	23.19	0.21	22.01	0.14	1.18	766.08	249.02	22.65	0.12	21.77	0.09	0.88
123.01.....	563.98	19.27	0.01	18.74	0.01	0.53	776.65	437.04	22.97	0.17	20.66	0.04	2.31
129.26.....	317.15	20.21	0.02	19.74	0.01	0.46	810.07	122.05	24.14	0.48	23.46	0.41	0.68
130.66.....	657.24	23.63	0.26	22.07	0.17	1.56	817.75	477.48	23.55	0.25	21.95	0.10	1.59
141.73.....	285.03	23.67	0.27	23.08	0.34	0.59	843.14	40.73	21.53	0.05	20.55	0.04	0.98
149.70.....	451.57	24.14	0.40	23.19	0.54	0.96	846.03	310.12	22.53	0.11	21.44	0.06	1.09
150.38.....	277.60	24.10	0.43	21.96	0.12	2.14	851.23	543.52	22.88	0.19	21.87	0.11	1.01
151.78.....	334.16	23.98	0.47	23.43	0.51	0.55	866.87	545.86	21.80	0.09	21.17	0.09	0.63
159.64.....	202.24	18.23	0.01	17.56	0.01	0.67	878.27	532.91	23.08	0.19	20.98	0.05	2.10
161.98.....	261.17	20.41	0.02	19.88	0.02	0.53	889.86	570.06	24.00	0.40	23.34	0.41	0.66
175.69.....	123.52	23.86	0.36	23.02	0.30	0.84	896.98	618.05	22.51	0.12	22.50	0.18	0.01
178.66.....	518.49	24.04	0.33	22.97	0.42	1.07	901.38	171.38	22.14	0.07	20.89	0.05	1.25
185.41.....	471.75	21.72	0.05	20.33	0.03	1.38	908.05	364.26	20.43	0.02	18.83	0.01	1.59
191.35.....	200.32	24.19	0.43	22.85	0.39	1.34	917.76	57.97	17.40	0.01	16.31	0.01	1.09
215.62.....	47.76	24.22	0.39	23.32	0.52	0.90	918.08	469.86	19.72	0.01	18.96	0.01	0.76
222.46.....	161.78	23.63	0.46	23.16	0.41	0.47	940.85	419.43	23.25	0.19	22.14	0.16	1.10
228.24.....	360.29	22.93	0.16	21.68	0.10	1.25	955.46	656.59	23.75	0.31	21.83	0.13	1.92
232.59.....	96.41	24.27	0.53	23.64	0.54	0.63	956.05	320.87	23.92	0.40	23.39	0.46	0.53
246.81.....	33.30	16.84	0.01	16.35	0.01	0.49	956.79	654.89	23.77	0.37	21.82	0.12	1.95
270.70.....	468.93	23.35	0.19	21.45	0.09	1.90	958.15	380.78	19.38	0.01	18.84	0.01	0.54
271.41.....	300.32	23.60	0.34	23.18	0.44	0.43	968.29	207.51	20.54	0.02	20.10	0.02	0.44
280.53.....	540.91	23.88	0.42	21.68	0.09	2.20	972.06	181.21	22.67	0.10	21.43	0.06	1.24
289.59.....	389.99	19.95	0.01	18.98	0.01	0.97	974.82	405.69	23.70	0.32	22.05	0.11	1.65
290.50.....	510.00	24.19	0.42	23.22	0.45	0.97	976.69	486.20	23.70	0.33	22.84	0.25	0.86
290.92.....	82.19	21.76	0.06	19.22	0.02	2.54	989.01	90.57	23.79	0.37	21.18	0.05	2.61
304.43.....	405.52	21.48	0.07	19.91	0.04	1.57	1005.43	68.97	21.83	0.09	20.46	0.05	1.37
309.07.....	607.91	24.26	0.43	23.52	0.50	0.74	1005.67	23.52	21.88	0.11	20.22	0.06	1.66
355.93.....	79.71	24.13	0.50	23.27	0.43	0.86	1010.28	61.51	21.85	0.06	19.81	0.03	2.04
356.78.....	384.78	23.05	0.19	21.01	0.04	2.04	1013.87	522.05	24.19	0.48	23.51	0.51	0.68
360.77.....	122.23	23.49	0.25	22.10	0.12	1.39	1023.80	70.93	23.65	0.25	22.16	0.19	1.49
390.10.....	538.87	22.42	0.12	20.67	0.05	1.75	1023.90	518.10	23.39	0.25	21.37	0.06	2.01
391.71.....	116.74	16.34	0.05	15.64	0.04	0.70	1029.53	619.88	21.56	0.04	21.15	0.06	0.41
391.85.....	573.53	23.09	0.18	21.73	0.10	1.36	1030.44	475.40	23.74	0.37	22.31	0.19	1.43
396.99.....	409.93	17.29	0.01	16.83	0.01	0.46	1035.16	416.25	22.58	0.12	21.60	0.07	0.97
401.62.....	41.31	17.78	0.01	17.21	0.01	0.57	1039.53	610.96	22.06	0.08	19.49	0.01	2.57
417.64.....	165.77	23.82	0.44	22.84	0.31	0.99	1045.45	448.48	23.85	0.34	22.60	0.17	1.25
417.67.....	264.74	22.59	0.12	20.81	0.05	1.78	1057.47	588.77	23.90	0.33	22.98	0.32	0.92
431.19.....	387.44	16.19	0.06	15.79	0.04	0.41	1076.08	344.36	23.82	0.37	23.42	0.49	0.41
446.92.....	227.94	20.93	0.03	20.51	0.03	0.42	1079.56	601.90	23.27	0.21	21.43	0.08	1.84
453.29.....	423.30	23.72	0.28	21.95	0.11	1.77	1087.40	438.94	22.61	0.13	21.87	0.09	0.75
480.55.....	545.63	21.55	0.05	19.36	0.02	2.19	1099.23	261.87	23.60	0.29	23.07	0.32	0.53
487.36.....	413.35	18.08	0.01	16.74	0.01	1.35	1099.47	102.35	23.86	0.30	21.87	0.10	2.00
501.17.....	269.66	23.21	0.20	21.13	0.06	2.08	1117.27	95.55	18.38	0.00	17.86	0.01	0.51
507.17.....	291.03	22.45	0.09	20.59	0.04	1.86	1128.81	215.10	23.85	0.38	22.01	0.11	1.84
509.84.....	522.19	20.44	0.02	20.04	0.02	0.40	1134.04	8.74	23.98	0.47	21.61	0.08	2.36
512.25.....	266.67	22.59	0.12	21.10	0.06	1.49	1157.39	86.25	23.98	0.35	22.45	0.21	1.53
574.02.....	477.68	23.66	0.28	22.57	0.20	1.08	1167.58	19.61	19.77	0.01	18.26	0.01	1.51
593.60.....	549.77	23.49	0.24	23.03	0.36	0.46	1185.34	37.68	22.85	0.16	21.28	0.07	1.57
600.03.....	344.42	19.52	0.01	18.72	0.01	0.80	1292.42	24.57	24.05	0.50	21.79	0.10	2.26
610.64.....	248.81	24.27	0.53	21.52	0.08	2.75	1292.57	22.77	23.92	0.44	21.80	0.10	2.12
618.29.....	244.10	20.54	0.02	19.80	0.02	0.75	1537.64	68.94	23.73	0.36	22.79	0.22	0.94
620.63.....	339.48	22.93	0.12	20.34	0.03	2.60	1555.28	60.56	16.42	0.03	15.61	0.05	0.81
623.14.....	650.07	22.85	0.13	20.94	0.04	1.91	1608.40	66.13	24.08	0.49	23.51	0.49	0.56
637.97.....	613.74	21.11	0.08	19.63	0.06	1.48	1626.19	5.55	22.29	0.14	21.64	0.09	0.65
640.10.....	302.71	20.54	0.02	18.65	0.01	1.89	1634.89	122.69	16.59	0.02	15.91	0.02	0.67
640.19.....	646.47	23.26	0.22	22.47	0.14	0.79	1670.17	55.69	16.08	0.04	15.52	0.05	0.56

The tip of the RGB is an excellent distance indicator⁵ (e.g., Lee 1993), having $M_I = -4.0$ for old and metal-poor populations. IC 5152 is known to have a low metallicity from its H II regions: $12 + \log(\text{O/H}) = 7.71$ (Hidalgo-Gámez & Olofsson 1998; see below). If the break at $I \approx 18.5 \pm 0.1$ were the RGB, the distance would be ~ 300 kpc, while the second break at $I = 20.4$ would yield 760 kpc. Both can be considered unlikely, for the following reasons:

1. The failure of adaptive optics observations to resolve stars in this galaxy gave a lower limit to the distance of 1.5 Mpc (Bedding et al. 1997). The Cepheids discovered by Caldwell et al. (1988) also rule out a small distance.

2. The presence of H II regions and UV bright stars (see below) indicates the presence of a young population. Therefore, the stellar population is expected to include young red supergiants.

3. At these distances, IC 5152 would be the smallest dwarf irregular galaxy known ($M_B = -10.7$ and -12.7 , respectively) and would be located away from the mean relation defined by its peers in the L versus $[\text{Fe}/\text{H}]$ plane.

We conclude that a consistent interpretation within the available data is reached if the two breaks are identified with the tip of the red supergiant sequence and the tip of the AGB. At a distance of $m - M_0 = 26.15$ (see below), the tip of the RGB would be found at $I = 22.2$ for $E_{V-I} = 0$, hidden by the incompleteness in the photometry.

⁵ A sparsely populated RGB can hide the actual tip of the RGB, giving the appearance of a break at a too faint magnitude. In this case the RGB loses its power as distance indicator, and the derived distance becomes an upper limit.

4. FUNDAMENTAL PARAMETERS OF IC 5152

4.1. The Distance and Total Luminosity of IC 5152

In the absence of a detected tip of the RGB, other, less accurate, distance indicators have to be used. We obtain the distance to IC 5152 by direct comparison with the color-magnitude diagrams of similar galaxies: the LMC (Shapley Constellation III, Reid et al. 1987), the SMC (Reid & Mould 1990), WLM (Minniti & Zijlstra 1997), and NGC 3109 (Minniti et al. 1999). These galaxies bracket the likely metallicity of IC 5152, as well as its total luminosity. The comparison with the last two galaxies is shown in Figure 10.

We find a difference $\Delta\mu$ of distance modulus of 7.6, 1.4, and 0.5 mag with the LMC, WLM, and NGC 3109, respectively. For $A_I = 0$, the distance modulus to IC 5152 is $m - M_0 = 26.15 \pm 0.2$, which translates into $D = 1.7$ Mpc. The error bar in the distance modulus includes a possible systematic uncertainty of 0.1 mag in the photometric zero point. The total luminosity for IC 5152 has been found to be $M_B = -14.5$ for $m - M_0 = 25.9$ (e.g., Huchtmeier & Richter 1986). With the present, more accurate distance determination, this should be revised to $M_B = -14.8$.

With this distance, the brightest red supergiants that are likely to be members of IC 5152 reach $M_{\text{bol}} = -9.5$. The termination of the AGB corresponds to a value of M_{bol} from -7.5 to -7.0 , in approximate agreement with the theoretical limit ($M_{\text{bol}} = -7.2$) for the most massive AGB stars. The termination of AGB stars near this limit is also seen in the LMC (e.g., Zijlstra et al. 1996). The observed range for the most luminous red supergiants is also in accordance with expectations (e.g., Chiosi & Maeder 1986) implying progenitor masses up to $50 M_\odot$.

At the low metallicity, this AGB may be dominated by carbon stars. The relation used for the bolometric magni-

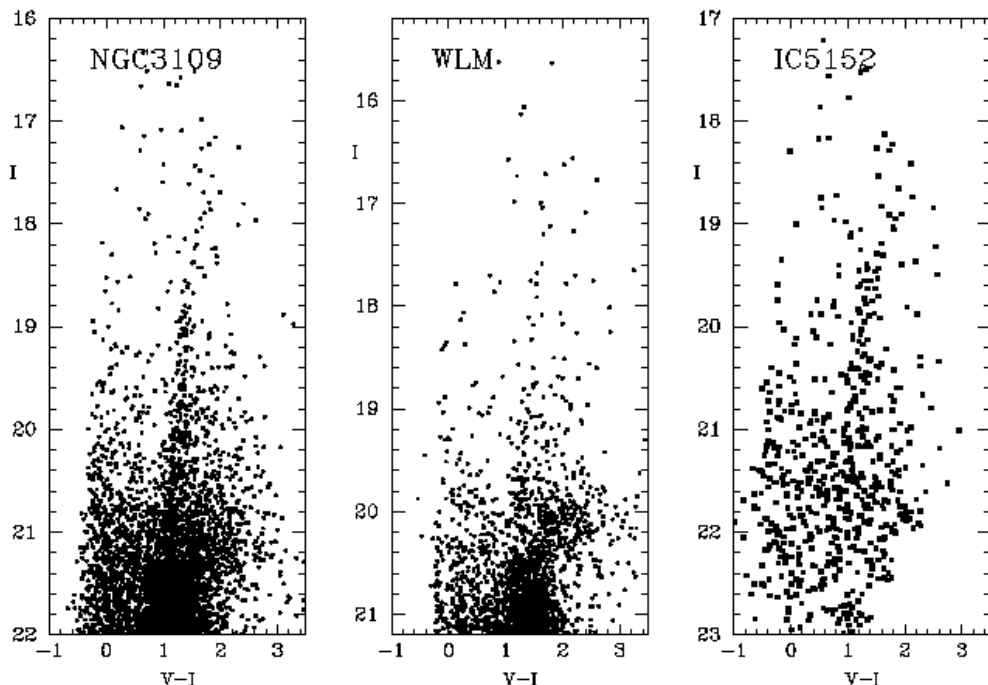


FIG. 10.—Comparison of IC 5152 with the color-magnitude diagrams of the dIrr galaxies NGC 3109 and WLM

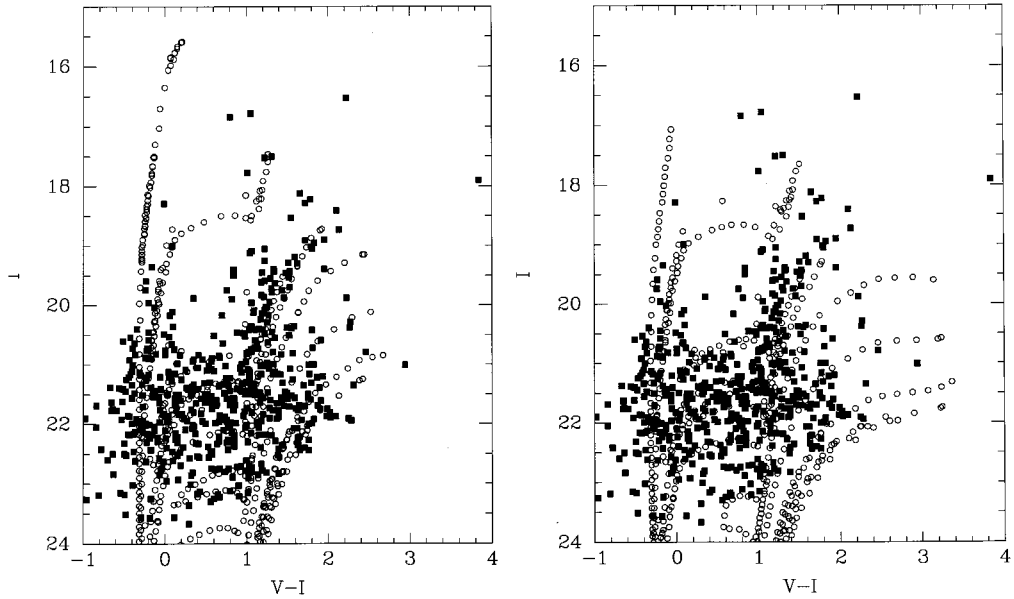


FIG. 11.— VI color-magnitude diagram for IC 5152 compared with the isochrones of Bertelli et al. (1994) for $Z = 0.001$ (left) and $Z = 0.004$ (right). The isochrones have been shifted according to $m - M = 26.15$ and $E_{V-I} = 0$ measured in this work. From top to bottom, the isochrones shown have ages $\log t = 6.6, 7.0, 7.8, 8.0, 8.7, 9.0, 9.7$ and 10.0 yr.

tude is slightly inappropriate for carbon stars (Brewer, Richter, & Crabtree 1995), but the carbon star contribution would only be important for the faintest magnitudes, where we are incomplete. At low metallicities, the brightest AGB stars may in fact again be oxygen-rich due to hot bottom burning, whereas lower on the AGB carbon stars dominate (e.g., van Loon et al. 1998). The peak AGB luminosity indicated in IC 5152 corresponds to a population of AGB stars with age $\sim 10^8$ yr.

4.2. Metal Abundances and Ages

The metallicity of old and metal-poor populations can be derived from the $V - I$ color of their RGB (e.g., Da Costa & Armandroff 1990). A similar technique can be applied to the color of the supergiant stars, since the theoretical isochrones predict that these stars will also get bluer as the metallicity decreases (Bertelli et al. 1994; Bressan, Chiosi, & Fagotto 1994). Unfortunately, metallicity and age are degenerate, producing similar effects in the optical color-magnitude diagrams. In order to avoid systematics, we then compare the color of the stars in the supergiant branch of IC 5152 with those of similar galaxies. As before, we chose the LMC, SMC, the WLM galaxy, and NGC 3109, which bracket the metallicity of IC 5152. The IC 5152 stars are about 0.05 mag redder than the corresponding stars in WLM and NGC 3109 (Fig. 10), indicating that they are more metal-rich in the mean.

The ages of old and intermediate-age stellar populations can be derived using the absolute magnitudes of their brightest red stars. If the photometry reaches beyond the red giant branch, the oldest populations can be studied (e.g., Lee 1993; Minniti & Zijlstra 1996, 1997). Since this is not the case here, we can only study the population of intermediate-age stars in the IC 5152 disk. Figure 11 shows the I versus $V-I$ color-magnitude diagrams for the southeast portion of the IC 5152 disk, along with the isochrones of Bertelli et al. (1994) corresponding to two different metallicities: $Z/Z_\odot = 0.05$ and 0.2 . In order to plot

the isochrones, we have assumed $m - M = 26.15$ and $E_{V-I} = 0$.

The color of the main sequence agrees with the isochrones, indicating that the reddening is nearly zero. The brightest stars are consistent with isochrones of $\log t = 7.0$ yr. The colors and magnitudes of the well-populated red supergiant branch overlaps the isochrones of $\log t = 7.8-8.0$ yr for $Z = 0.001$, being slightly bluer than the corresponding $Z = 0.004$ isochrones. Stars with intermediate colors (yellow stars with $0.2 < V-I < 1.0$) should be stars doing blue loops according to the isochrones. These yellow stars appear in large numbers at $I > 21.0$. Above $I = 21.0$ there is a clear separation between the main sequence and the supergiant branches. This is evidence of a large population of stars with ages $\log t > 7.8$ yr, consistent with the presence of Cepheid variables (Caldwell, Schommer, & Graham 1988). Some of the reddest stars with $V-I > 1.5$ overlap the older isochrones with $\log t = 9.0$ to 10.0 yr, showing that old stars are also present.

This interpretation depends on the adopted distance, which cannot be uniquely obtained from the isochrones alone; the isochrones can be shifted upward without invalidating the fit. The additional data discussed above is needed to constrain the possible distance range.

The reddest stars reach $V-I = 2.5$, bluer than the extremes predicted by the $Z = 0.004$ isochrones ($V-I = 3.4$). There are a few red stars that are redder than the $Z = 0.001$ isochrones would predict, indicating that $0.001 < Z < 0.004$. Likewise, the LMC supergiant branch is more extended to the red than the IC 5152 supergiant branch. From this comparison with the isochrones and with the color-magnitude diagrams of similar galaxies, we conclude that the intermediate-age stellar component of the IC 5152 disk has a metallicity $Z = 0.002$.

The central region of this galaxy was observed with the Faint Object Camera (FOC) on the *Hubble Space Telescope* (*HST*) in the ultraviolet. We have retrieved the FOC image from the *HST* archives, in order to make a comparison with

our optical images of the same region. This image taken with the F220W filter is centered at $\alpha = 22^{\text{h}}02^{\text{m}}41^{\text{s}}90$, $\delta = -51^{\circ}17'44''.0$ (J2000.0) and covers $22'' \times 22''$. It shows obvious star-forming activity in the form of numerous ultraviolet point sources, which are probably O- and B-type stars (Maoz et al. 1996). There is no obvious bright nucleus present in this field. Figure 11 shows the V - and I -band NTT images of the central $30'' \times 30''$, for comparison with Fig. 2 (Pls. 37–47) of Maoz et al. (1996). Most of the ultraviolet sources can be identified with optical sources seen in the V -band image. The sources in common have blue $V - I$ colors, and some are clearly blends of 2–3 stars due to the lower resolution of the NTT images compared with the *HST* ones.

The brightest and reddest source in Figure 11 (located at $X = 1707.98$, $Y = 599.31$, with $I = 18.12$ and $V - I = 1.65$) has a faint counterpart in the FOC image. If it is an unreddened single red supergiant, it would have $M_{\text{bol}} = -7.5$, but it should not show any ultraviolet counterpart. The ultraviolet detection indicates that it could be a compact stellar cluster. This source is located in the geometric center of IC 5152 judging from the Palomar Observatory Sky Survey (POSS) plates, and we suggest it could be the highly reddened nucleus of this galaxy.

5. OTHER POPULATION TRACERS

5.1. Star Clusters in IC 5152

The status of globular cluster research in galaxies of the Local Group is summarized by Olszewski (1994). IC 5152 does not have any globular clusters known. We have searched for globulars clusters within a defined magnitude and color range, looking for objects that are nearly resolved (i.e., $\text{FWHM} \geq \text{FWFM}_{\text{psf}}$). For $m - M = 26.15$ and $E(V - I) = 0$, the magnitude and color range of possible globulars was taken to be $22 > I > 16.5$, and $0.7 \leq V - I \leq 1.2$, respectively, from Reed (1985) and Harris (1996). Even though the resolution is not good enough to allow to discriminate the presence of fainter clusters from chance overlapping of individual unrelated stars, we find 10 objects brighter than $I \approx 20$ that have color similar to Galactic globulars. Based on the field color-magnitude diagram shown in Figure 6, we would have expected four such objects (although the field itself can contain IC 5152 globulars if the cluster system of this galaxy is extended). Of the 10 candidates, six have colors and magnitudes consistent with blends between a bright main-sequence star and a bright red supergiant star. The rest, however, cannot be explained in this way because they are too bright.

5.2. Carbon Stars

No systematic search for C stars has been made in IC 5152. The C star luminosity functions given by Brewer, Richer, & Crabtree (1995) for M31 and by Richer (1981) for the LMC bar west field peak at $M_I = -4.4$, with a total range of about $-3.4 \leq I_0 \leq -5.0$. C stars are expected to be very red, with $2 < V - I < 3$. These expected magnitudes and colors are coincident with the location of the reddest stars seen in the lower portion of the color-magnitude diagram of IC 5152 (Fig. 5). Since these stars are located within the main body of the galaxy, we conclude that there is a substantial number of candidate C stars in this galaxy.

It is interesting to note that IC 5152 was detected by *IRAS* (source identification IRAS 21594–51). Saunders et

al. (1990) measured a total luminosity at $60 \mu\text{m}$ of $\log L_{60}/L_{\odot} = 7.48$ for this galaxy, adopting a distance $D = 1.5 \text{ Mpc}$. We suggest that part of this emission (of order 1 Jy at $12 \mu\text{m}$) could be due to circumstellar shells from mass-losing carbon stars in this galaxy. Most of the *IRAS* flux may, however, be due to the H II regions, as has been found for the dwarf irregular galaxy NGC 6822 (Israel, Bontekoe, & Kester 1996).

5.3. H II Regions

Being a late-type galaxy, Sdm IV–V, IC 5152 is reasonably active at forming stars at the present time (e.g. Elmegreen et al 1994). From the main sequence (Fig. 12), we see that the youngest stars are $\sim 10^7 \text{ yr}$ old, indicative of ongoing star formation. The H II regions of IC 5152 have been studied by Talent (1980) and by Webster et al. (1983). The former data are not published, but the result is quoted (Skillman, Kennicutt, & Hodge 1989; Marconi et al. 1994; Lisenfeld & Ferrara 1998) as $12 + \log (\text{O/H}) = 8.36$. Webster et al. derive $12 + \log (\text{O/H}) = 8.4$ for a single H II region. However, Hidalgo-Gámez & Olofsson (1998) derive a rather lower abundance of $12 + \log (\text{O/H}) = 7.71$, based on the data of Webster et al.

The color-magnitude diagram indicates that the stellar component of the IC 5152 disk has a metallicity $Z = 0.002$, in approximate agreement with the oxygen abundances listed by Hidalgo-Gámez & Olofsson (1998). It is reasonable to assume that young supergiants and H II regions will have the same metallicity. Galaxies with a relatively young population are less likely to show a high value of [O/Fe] (e.g., Walsh et al. 1997) so that we find better consistency with Hidalgo-Gámez & Olofsson (1998).

Skillman et al. (1989) point out that IC 5152 falls well away from the relation defined by other dwarf galaxies in the $12 + \log (\text{O/H})$ versus M_B plane. This galaxy is the most discrepant point in their sample, being too faint and/or too metal-rich. The more accurate distance presented here somewhat alleviates this problem, but not enough to bring IC 5152 into agreement with the metallicity-luminosity relation followed by other dwarfs. However, the discrepancy disappears when using the lower abundance published by Hidalgo-Gámez & Olofsson (1998), which is supported by the metallicity of the stellar component in IC 5152. (Note that Lisenfeld & Ferrara (1998) use an extreme distance of 3.0 Mpc, and Hidalgo-Gámez & Olofsson (1998) use 2.3 Mpc, shifting IC 5152 off the relation in both studies.)

Further observations would be desirable, since the preferred value for the oxygen abundance is based on a single H II region for which two discrepant abundance determinations exist. The possibility that recent enrichment has caused metallicity variations within the gaseous disk can also not be ruled out. At the smaller distances of 300 and 760 kpc, the galaxy would fall far above the expected relation even for the reduced oxygen abundance, which is one of the arguments to prefer the larger distance of 1.7 Mpc.

5.4. Planetary Nebulae

No planetary nebulae in IC 5152 have been reported in the literature. Given the luminosity of this galaxy $M_B = -14.8$, we expect about 10 planetary nebulae to be present. If planetary nebulae could be found, they would allow for accurate oxygen abundance determinations for the intermediate-age stellar population.

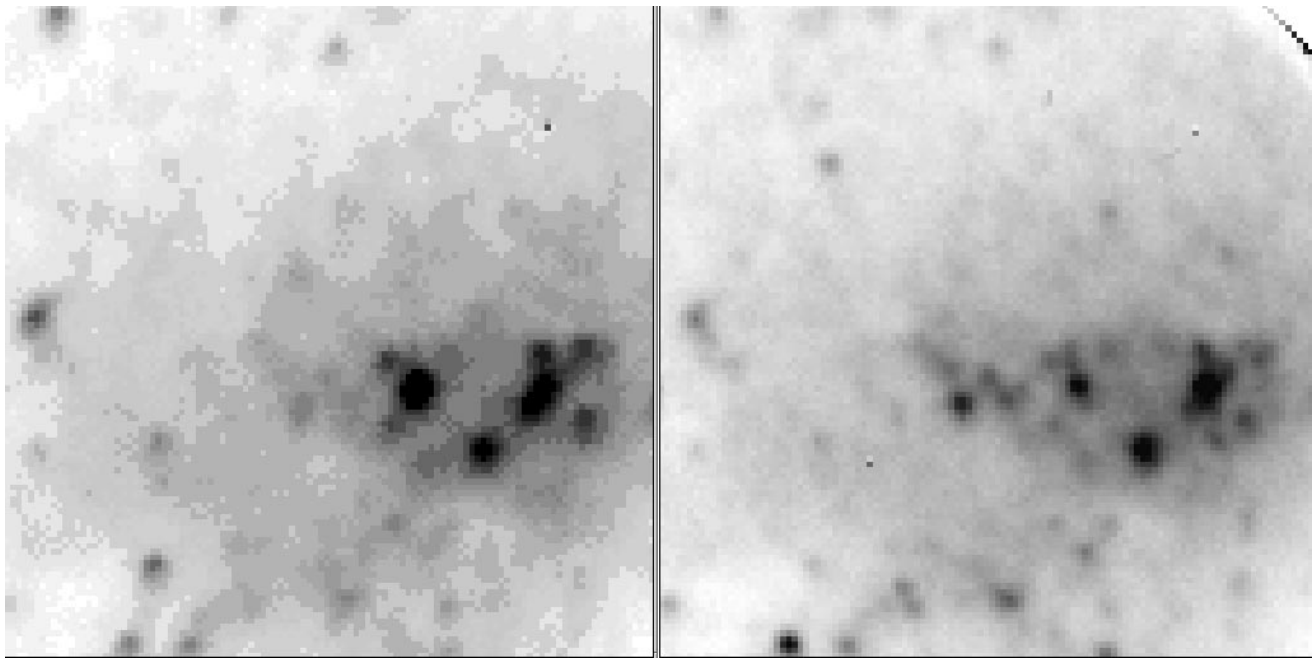


FIG. 12.—Central *I*-band (*left*) and *V*-band (*right*) images of IC 5152 covering $30'' \times 30''$. Compare these images with Plate 1 of Maoz et al. (1996). North is up, and east to the left. Most of the sources seen in the *V*-band image have ultraviolet counterparts, indicating that this region has active star formation. The brightest source in the *I*-band image is very faint in the ultraviolet, and could be the highly reddened nucleus of this galaxy.

5.5. Cepheid Variables

The only systematic search for Cepheid variables in IC 5152 reported in the literature is that of Caldwell et al. (1988). The distance modulus inferred from these data is $m - M_0 = 26.0$ (see van den Bergh 1994a), corresponding to $D = 1.6$ Mpc, in agreement with the distance obtained in the present work.

5.6. The Gaseous Component: H II Observations

Dwarf galaxies have dark matter halos, their total M/L being larger than that of normal spiral galaxies (e.g., Carignan & Freeman 1988; Côté 1995), and IC 5152 seems to be no exception. H I measurements for IC 5152 are given by Huchtmeier & Richter (1986). They list a velocity of $V_{LG} = +53$, a diameter of $A = 1.95$ kpc (or $A = 2.1$ kpc using our revised distance), and infer $M_T/L_B = 3.5$.

6. GALAXY GROUP ASSOCIATION

Our main result is that the distance of $D = 1.7$ Mpc would place IC 5152 outside the accepted boundaries of the Local Group. The distance, together with the small positive velocity with respect to the Local Group, implies that this galaxy is just turning around from the Hubble flow (Peebles 1995).

In the $\cos \theta$ versus velocity diagram, as commented by van den Bergh (1994b), the position of IC 5152 is only barely outside the region occupied by most certain members of the Local Group. Thus, its membership is still uncertain even with the improved distance estimate. IC 5152 is at a distance of 1.6 Mpc from the center of the Local Group, at right angles to the direction of M31. Using a mass of the Local group of $4 \times 10^{12} M_\odot$ indicates that its radial velocity is less than the escape velocity; however, the tangential velocity is not known and may be dominant: a circular orbit would require approximately $v_t = 100$ km s $^{-1}$.

The mass distribution outside the Local Group also plays a role in the membership problem. IC 5152 is, in fact, closer to NGC 300 in the Sculptor Group (1.2 Mpc) than to the main galaxies in the Local Group. The Sculptor Group has been found to have a large population of dwarf galaxies (Côté et al. 1997), although their survey did not cover the area of IC 5152. The result of Côté et al. (1997) shows that the catalogues of dwarf galaxies beyond 1 Mpc is still very incomplete. It is, therefore, possible that more such isolated dwarfs in-between the two groups exist, and even a common halo of dwarfs could be envisaged.

There are no other known galaxies in this direction at this approximate distance. The dwarfs WLM, Tucana, and NGC 1613 are in the same quadrant but are much closer than IC 5152, being real members of the Local Group (van den Bergh 1994b). IC 5152 appears to be one of the most isolated nearby dwarf galaxies known, located in-between the Sculptor and Local Groups but distant enough to have so far evolved without interaction with either of these groups. The question arises what drives the star formation in such an isolated galaxy. The presence of numerous UV-bright stars in the central regions suggests a relatively high rate of star formation, showing that star formation in dwarf galaxies does not require external disturbances. It has been suggested by van den Bergh (1994b) that for the smallest dwarf galaxies ($M_B > -14.0$) the star formation history depends on the distance to a large galaxy, with the nearest galaxies having most of their star formation at an early phase and more isolated dwarfs have a higher fraction of recent star formation. IC 5152 may form an extreme case of the latter.

7. CONCLUSIONS

We have presented *VI* photometry for 553 stars in the field of the dwarf irregular galaxy IC 5152, a suspect member of the Local Group, and have made the first CCD

color-magnitude diagrams and luminosity functions obtained for this galaxy.

By direct comparison of the VI color-magnitude diagram with those of similar galaxies, we derive a distance modulus of $m - M_0 = 26.15 \pm 0.2$ for this galaxy. The distance of $D = 1.7$ Mpc places IC 5152 just outside the accepted boundaries of the Local Group, leaving its membership open.

Based on the color-magnitude diagrams, we have explored the stellar population content, metallicities, and ages for the main body of IC 5152. The main sequence suggests that significant numbers of young stars are present in this galaxy, and the extent of the supergiant and asymptotic giant branches suggests the presence of intermediate-age stars with metallicity $Z \approx 0.002$, lower than previously suggested. The present result places the galaxy on the luminosity-metallicity sequence of dwarf galaxies of Skillman et al. (1989). The central region is an active site of star formation, as found by comparing our optical photometry

with *Hubble Space Telescope* ultraviolet images. On the basis of the ultraviolet and optical images we identify a candidate for a potential nucleus. A few globular cluster candidates are found, which need to be confirmed spectroscopically.

We also construct deep I -band luminosity functions and a bolometric luminosity function for the red stellar component of this galaxy. Based on these we confirm the presence of an intermediate-age stellar population of AGB stars and estimate that the brightest red supergiants reach $M_{\text{bol}} = -9.5$ mag.

We are grateful for the remote-control operators J. Rodriguez and V. Reyes, and the telescope operator M. Pizarro, for their efficiency and expertise at the NTT. This work was performed in part under the auspices of the US Department of Energy by Lawrence Livermore National Laboratory under Contract W-7405-Eng-48.

REFERENCES

- Bedding, T., Minniti, D., Courbin, F., & Sams, B. 1997, A&A, 236, 936
 Bertelli, G., Bressan, A., Chiosi, C., Fagotto, F., & Nasi, E. 1994, A&AS, 106, 275
 Bessell, M. S., & Wood, P. R. 1984, PASP, 96, 247
 Bottinelli, L., Gouguenheim, L., Paturel, G., & de Vaucouleurs, G. 1984, A&AS, 56, 381
 Bressan, A., Chiosi, C., & Fagotto, F. 1994, ApJS, 94, 63
 Brewer, J. P., Richer, H. B., & Crabtree, D. R. 1995, AJ, 109, 2480
 Burstein, D., & Heiles, C. 1984, ApJS, 54, 33
 Caldwell, N., Schommer, R. A., & Graham, J. 1988, PASP, 100, 1217
 Carignan, C., & Freeman, K. 1988, ApJ, 332, L33
 Chiosi, C., & Maeder, A. 1986, ARA&A, 24, 239
 Côté, S. 1995, Ph.D. thesis, Australian Natl. Univ.
 Côté, S., et al. 1997, AJ, 114, 1313
 Da Costa, G. S., & Armandroff, T. E. 1990, AJ, 100, 162
 Dohm-Palmer, R. C., Skillman, E. D., Saha, A., Tolstoy, E., Mateo, M., Gallagher, J., Hoessel, J., Chiosi, C., & Dufour, R. J. 1997, AJ, 114, 2514
 Elmegreen, D. M., Elmegreen, B. G., Lang, C., & Stephens, C. 1994, ApJ, 425, 57
 Gallart, C., Aparicio, A., Chiosi, C., Bertelli, G., & Vilchez, J. M. 1994, ApJ, 425, L9
 Gallart, C., Aparicio, A., & Vilchez, J. M. 1996, AJ, 112, 1928
 Grebel, E. K. 1998, in IAU Symp. 192, The Stellar Content of Local Group Galaxies, ed. P. Whitelock & R. Cannon (San Francisco: ASP), 1
 Greggio, L., Marconi, G., Tosi, M., & Focardi, P. 1993, AJ, 105, 894
 Harris, W. 1996, AJ, 112, 1487
 Hidalgo-Gámez, A. M., & Olofsson, K. 1998, A&A, 334, 45
 Hog, E., Kuzmin, A., Bastian, U., Fabricius, C., Kuimov, K., Lindegren, L., Makarov, V. V., & Roeser, S. 1998, A&A, 335, L65
 Huchtmeier, W., & Richter, O. G. 1986, A&AS, 63, 323
 Israel, F. P., Bontekoe, T. R., & Kester, D. J. M. 1996, A&A, 308, 723
 Lisenfeld, U., & Ferrara, A. 1998, ApJ, 496, 145
 Landolt, A. U. 1992, AJ, 104, 340
 Lee, M. G. 1993, ApJ, 408, 409
 Maoz, D., Filippenko, A. V., Ho, L. C., Macchetto, F. D., Rix, H.-W., & Schneider, D. P. 1996, ApJS, 107, 215
 Mateo, M. 1998, ARA&A, 36, 435
 Marconi, G., Matteucci, F., & Tosi, M. 1994, MNRAS, 270, 35
 Minniti, D., & Zijlstra, A. A. 1997, AJ, 114, 147
 ———. 1996, ApJ, 467, L13
 Minniti, D., Zijlstra, A. A., & Alonso, M. V. 1999, AJ, 117, 881
 Olszewski, E. W. 1994, in IAU Symp. 164, Stellar Populations, ed. G. Gilmore & P. van der Kruit (Dordrecht: Kluwer), 181
 Peebles, P. J. E. 1995, ApJ, 449, 52
 Ratnatunga, K. U., & Bahcall, J. N. 1985, ApJS, 59, 63
 Reed, C. B. 1985, PASP, 97, 120
 Reid, N., & Mould, J. 1990, ApJ, 360, 490
 Reid, N., Mould, J., & Thompson, I. 1987, ApJ, 323, 433
 Richer, H. B. 1981, ApJ, 243, 744
 Rieke, G. H., & Lebofsky, M. J. 1985, ApJ, 288, 618
 Sandage, A. 1986, ApJ, 307, 1
 Sandage, A., & Bedke, J. 1985, AJ, 90, 1992
 Saunders, W., Rowan-Robinson, M., Lawrence, A., Efstathiou, G., Kaiser, N., Ellis, R. S., & Frenk, C. S. 1990, MNRAS, 242, 318
 Skillman, E. D., Kennicutt, R. C., & Hodge, P. W. 1989, ApJ, 347, 875
 Stetson, P. B. 1987, PASP, 99, 191
 Talent, D. L. 1980, Ph.D. thesis, Rice Univ.
 Tolstoy, E. 1995, Ph.D. thesis, Univ. Groningen
 Tolstoy, E., & Saha, A. 1996, ApJ, 462, 672
 Tosi, M. 1994, in Dwarf Galaxies, ed. G. Meylan & P. Prugniel (Garching: ESO), 465
 Tyson, J. A. 1988, AJ, 96, 1
 van den Bergh, S. 1994a, AJ, 107, 1328
 ———. 1994b, ApJ, 428, 617
 van Loon, J. T., Zijlstra, A. A., Whitelock, P. A., te Lintel Hekkert, P., Chapman, J. M., Loup, C., Groenewegen, M. A. T., Waters, L. B. F. M., & Trams, N. R. 1998, A&A, 329, 169
 Walsh, J. R., Dudziak, G., Minniti, D., & Zijlstra, A. A. 1997, ApJ, 487, 651
 Webster, B. L., Longmore, A. J., Hawarden, T. G., & Mebold, U. 1983, MNRAS, 205, 643
 White, S. D. M., & Rees, M. J. 1978, MNRAS, 183, 341
 Zijlstra, A. A., Loup, C., Waters, L. B. F. M., Whitelock, P. A., van Loon, J. T., & Guglielmo, F. 1996, MNRAS, 279, 32
 Zijlstra, A. A., Minniti, D., & Brewer, J. 1997, Messenger, 90, 19
 Zijlstra, A. A., Wallander, A., Kaper, L., & Rodriguez, J. A. 1997, PASP, 109, 1256